Imaging-based profiling for elucidation of antibacterial mechanisms of action

Anna A. Baranova[1], Vera A. Alferova[1,2], Vladimir A. Korshun[1], Anton P. Tyurin[1,*]
1. Shemyakin-Ovchinnikov Institute of Bioorganic Chemistry, Russian Academy of Sciences, 16/10 Miklukho-Maklay str., 117997, Moscow, Russia;
2. Belozersky Institute of Physico-Chemical Biology, Lomonosov Moscow State University, Leninskie Gory 1, 119234 Moscow, Russia;
* corresponding author: Dr. Anton P. Tyurin, anton2rin@gmail.com

Abstract

In this review, we aim to summarize experimental data and approaches to identifying cellular targets or mechanisms of action of antibacterials based on imaging techniques. Imaging-based profiling methods such as bacterial cytological profiling, dynamic bacterial morphology imaging and others have become a useful research tool for mechanistic studies of new antibiotics as well as combinations with conventional ones and other therapeutic options. The main methodological, experimental details and obtained results are summarized and discussed. The review covers the literature up to Feb 2024.

Keywords: antibacterials; antibiotics; bacterial phenotype; bacterial imaging; mechanism of action; fluorescent microscopy.

Introduction

The search for and development of new antibiotics today is impossible without elucidation or at least experimental confirmation of their mechanism of action and cellular target [1,2]. When we refer to a “target”, we are talking about partner biomolecules that are involved in either covalent or non-covalent binding to the antibiotic. The term “Mechanism of action” (MoA), as a more general concept, refers to the type of cellular process that the antibiotic disrupts. Although such an understanding is not a legislative requirement for substances newly introduced into medical practice, nevertheless, in the professional community there is a deep conviction about the necessity and practical value of this information [3]. Indeed, comprehending the mechanism makes it possible to predict the spectrum of activity of the substance, its possible toxic effect and many other parameters. Without understanding them, expensive and time-consuming preclinical and clinical trials are an extremely risky endeavor.

Traditional phenotypic screening remains the primary and most productive approach to the search for antibiotics [4,5]. “Phenotypic” in this context means a type of screening aimed at identifying substances that change the phenotype of a bacterial cell in a desired way: i.e., primarily, reducing its viability and/or growth rate. The main problem with this approach is precisely the lack of information about the mechanism underlying the observed phenotypic changes. To solve this problem, various approaches have been developed to elucidate the mechanism of action, both newly developed [3,6–8] and conventional, or "classical" ones. The “gold standard” for establishing the mechanism of action of an antibiotic is a macromolecular synthesis assay utilizing radioactively labeled precursors [9,10] (Fig. 1). However, this method, in addition to a number of practical problems associated with manipulating radioactive substances, has the disadvantage of not allowing reliable determination of all types of inhibition. This limitation arises because the action of an antibacterial agent is not always directly related to the inhibition of the biosynthesis of DNA, RNA, proteins, fatty acids or peptidoglycan. Consequently, the development of alternative approaches for determining the mechanism of action is an urgent task [11].

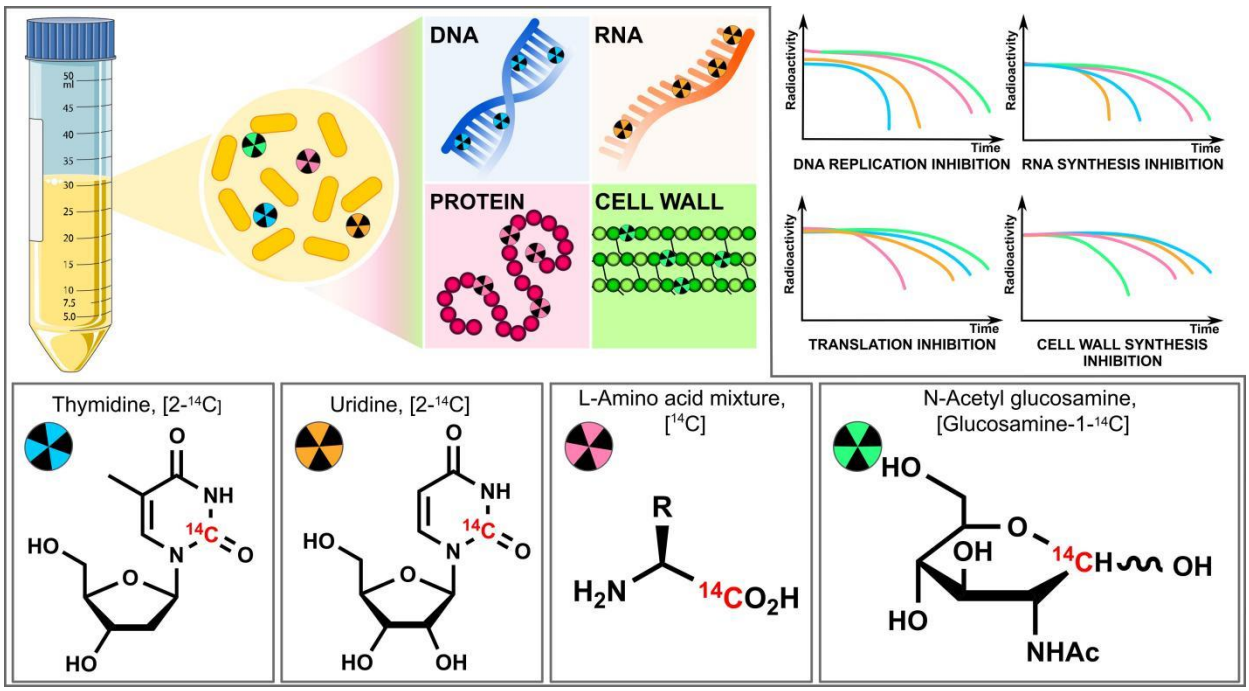

Fig.1. Macromolecular synthesis assay

In this review, we aimed to provide an analytical digest of experimental data and approaches for identifying cellular targets based on bacterial imaging. Imaging-based profiling and elucidation of the mechanism of action of a substance on a cell was proposed in a pioneering work [12]. But for a long time, a similar approach could not be applied to bacteria. The fact that antibiotics cause phenotypic changes in sensitive cells was reported at the dawn of the antibiotic research era, the 1940s. [13–15] Interestingly, these observations were made at a time when not only there was no understanding of the mechanism of action of antibiotics, but the complex structure of the bacterial cell remained terra incognita in many ways. Despite all these prerequisites and the successful use of cytoprofiling on cultures of eukaryotic cells (including yeasts) [16,17], it was not until 2012-2013 that a technique for bacterial cytological profiling (BCP) was introduced [18,19].

The key stages of the BCP method are presented in Fig. 2. First stage involves sample preparation, staining and imaging. Typically, cells in the mid-log phase are used to minimize cell heterogeneity and simplify the resulting picture. To obtain a more detailed images the fluorescent dyes are usually added to the samples. Subsequently, the aquired images undergo processing, wherein the intensities are normalized and bacterial cells are segmented (i.e. distinguished from the background and artifacts). The bacterial phenotype can be represented as a set of measurable parameters. For example, the length, width and area of the membrane, the length, width, area and number of nucleoids, and various ratios of such extractable features. So, the feature extraction and data analysis constitute the next key stage of BCP workflow.

The conceptual basis of the method is that phenotypic changes are weakly dependent on a specific effect. Stress can be caused by substances of various structures, factors regulating the expression of certain proteins (knockdown/overexpression), environmental factors (osmotic stress, bacteriophages, etc.). Moreover, phenotypic alterations strongly depend on the mechanism of action (MoA) of a given substance or factor. The detailed mechanism of this relationship continues to remain unclear, and the theory linking the macroscopic phenotype and biochemical stress under the influence of an antibiotic is under development [20–24]. However, it can be confidently stated that the connection between

the observed morphology of bacteria and the mechanism of action of the substance is rooted in the intricate interplay of all cellular processes [25] and is substantiated by experimental evidence.

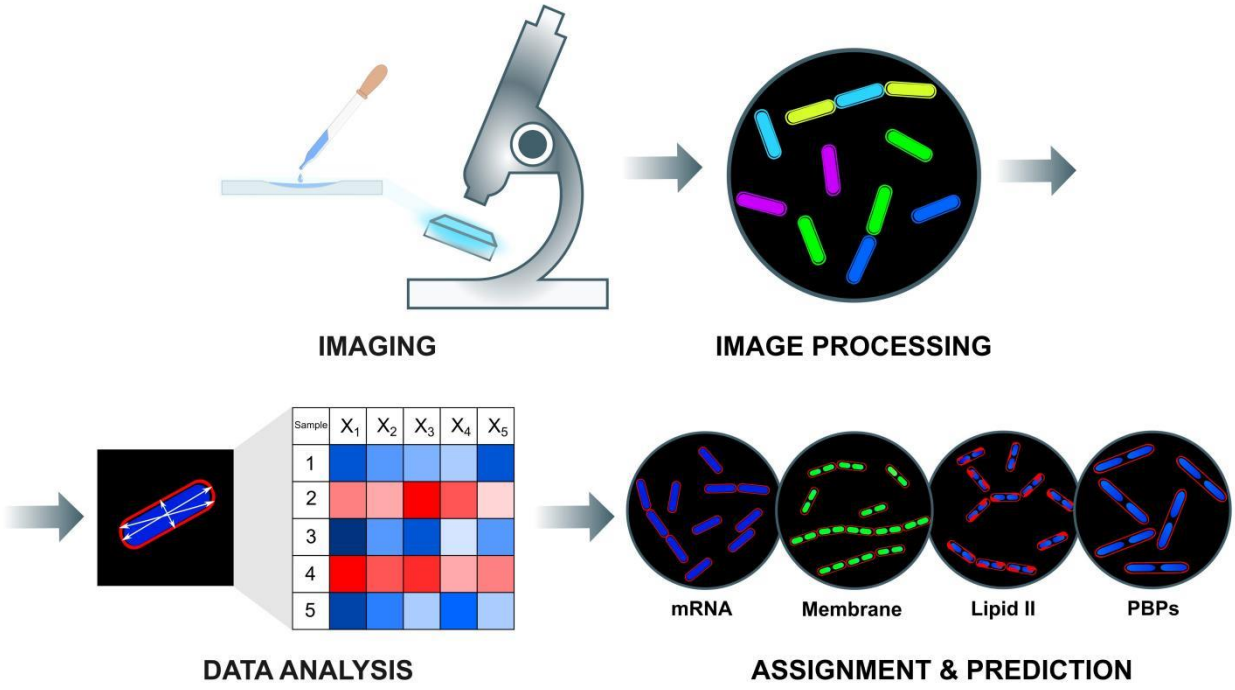

Fig. 2. Main steps of bacterial cytological profiling

Over the past 12 years, advancements in the application of BCP and similar methods in antibiotic research have received only brief mention in review articles covering other topics [6,26,27]. That is why we consider it necessary to conduct a more comprehensive and critical examination of the accumulated data.

Methodology

The search and preliminary selection of sources was carried out using the Web of Science, Google Scholar and PubMed search platforms using keyword combinations ("bacterial cytological profiling", "bacterial morphoprofiling", "image-based antibacterial drug profiling", "dynamic bacterial morphology imaging"), along with and cross-references. The inclusion criteria were:

1. Use of the bacterial cytological profiling methodology described above or one similar in basic parameters.

2. Primary use of imaging for profiling and/or elucidation the mechanism of action of a substance or other object of study. Publications where cytoprofiling or another analogous method were utilized for alternative purposes (for example, as in [28],to determine the sensitivity of bacteria to antibiotics) were excluded.

3. Publication type: article in a peer-reviewed journal. Abstracts and conference materials, monographs and book chapters, preprints were excluded from consideration.

As a result, a total of 89 publications meeting these criteria for the period from 01.2012 to 02.2024 were selected and are presented in Appendix A.

Data extraction and analysis

After further examination of all selected articles, the following information was extracted:

- The presented phenotypic profiling methodology was categorized as either original or an addition to a previously described methodology (see column “Base method”, Appendix A);

- The dyes or tags used to visualize bacteria in each study were recorded and listed in the corresponding column of Appendix A;

- The test cultures utilized for profiling and studying the mechanism of action were documented for each article and included in the "Test culture" column of Appendix A;

- The mechanism of action of the substances or other objects studied using image-based profiling was identified and detailed in the "Object of study" column of Appendix A;

- The main conclusions obtained by the authors as a result of applying the described method were summarized and outlined in the "Main results" column of Appendix A.

It is important to highlight the significant milestones in the development of the bacterial image-based profiling methodology. Initially, the effectiveness of the method was shown on conventional antibiotics and typical gram-positive (*B. subtilis*) [18] and gram-negative (*E. coli*) [19] test cultures. Subsequently, it was shown in [29] that an effect identical to that of the inhibitor can be achieved due to inducible degradation of a target protein. This combination of inhibition and subsequent profiling is promising for the search for selective inhibitors of those targets that have not yet been studied and are not involved in the development of new antibiotics. A similar methodology was used in [30] to search for inhibitors of msbA (lipopolysaccharide transporter important for outer membrane functioning in gram-negative bacteria). In [31], a method akin to BCP was proposed for profiling and determining the mechanism of action of anticancer drugs.

The work [32] highlights the observation that exposure to combinations of antibiotics often results in a complex array of combined phenotypes. This approach may be interesting as a more informative alternative to the traditional checkerboard assay for studying the interactions of various antimicrobial agents. On the other hand, this poses the task of more thorough analysis of a large number of images, which is impossible without automation and machine learning methods.

For the first time, the problem of classifying the mechanism of action of substances by bacterial phenotype was solved using machine learning methods in [33]. New analysis pipelines for both gram-negative bacilli and gram-positive cocci were proposed in [34]. With their help, the heterogeneity of phenotypic changes in Salmonella cells under ciprofloxacin exposure was shown [35]. Another semi-automated workflow named Antibiotic Drug screening and Image Characterization Toolbox (A.D.I.C.T.) was developed [36]. Of course, the use of automation methods for analyzing a large number of cells and machine learning algorithms for solving clustering and classification problems opens up new opportunities for further successful use of morphoprofiling [27,37]. However, none of the mentioned semi-automated workflows have yet received widespread adoption in the study of new antibacterial agents. Perhaps the availability of open-source tools [38] and their integration into widely used open image processing platforms such as ImageJ may eventually shift the landscape, leading to broader utilization of modern machine learning methods for addressing these challenges.

One of the new directions is the use of data on the dynamics of individual cells, implemented in the Dynamic Bacterial Morphology Imaging (DBMI) method [39]. This methodology employs quantitative time-lapse fluorescence imaging to elucidate the mechanism of action of antibiotics more rapidly and accurately. However, its implementation requires additional experimental techniques and sophisticated data analysis. The method has been recently applied to study the mechanism of antibacterial action of the natural polyketide harzianic acid [40].

For cytoprofiling the most commonly used imaging method is confocal fluorescence microscopy, which involves the use of selective fluorescent dyes:

1. Dyes that selectively stain nucleoid/nucleic acids;

2. Dyes that specifically stain the cell membrane;

3. Dyes that enable differentiation between intact (living) cells and damaged (dead) cells;

4. Other dyes and labels, among which cell wall imaging is most often used.

The structures of the dyes employed for phenotypic profiling purposes and those mentioned in Appendix A are shown in Fig. 3.

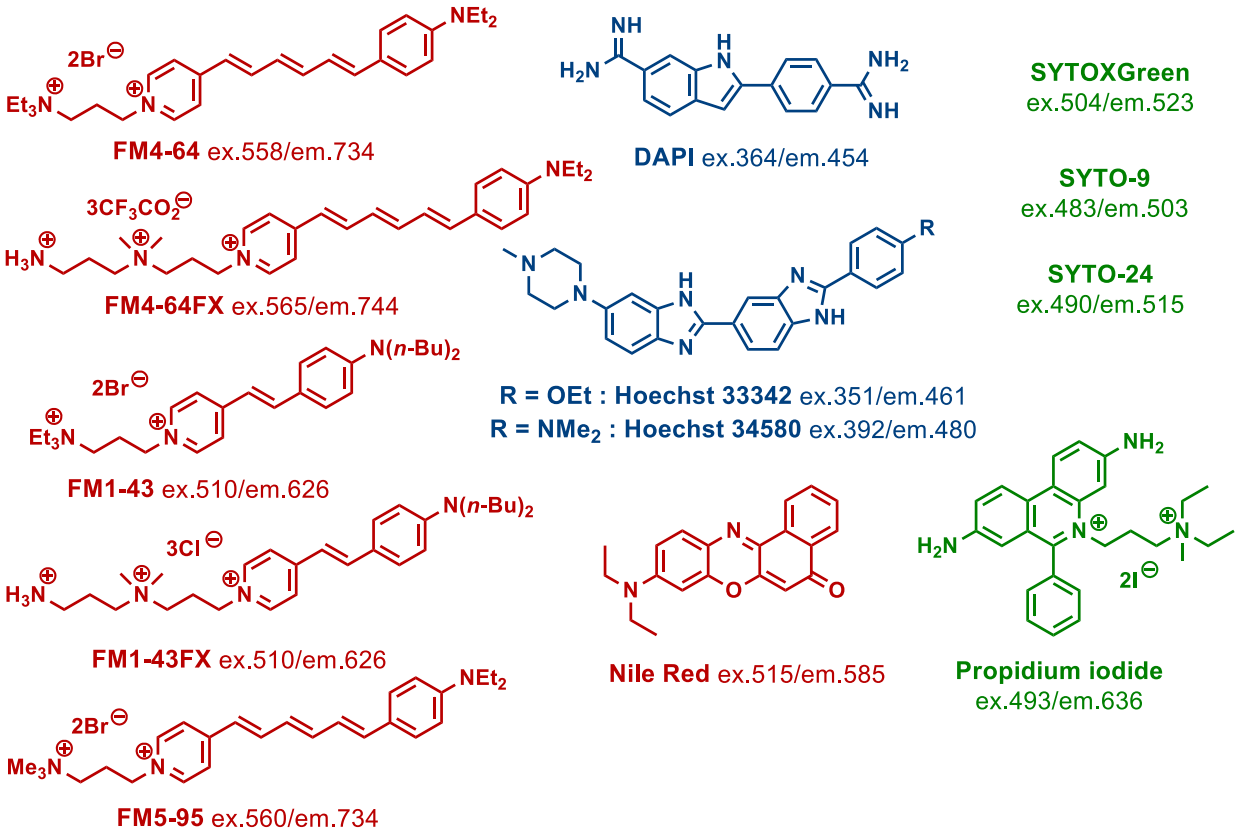

Fig. 3. Fluorescent dyes used in bacterial cytoprofiling. Different types of dyes are marked by different colours (see description above): 1-blue, 2-red, 3-green. For all compounds, the excitation and emission maxima in nm are given.

The most commonly used combination includes FM4–64, SYTOXGreen and DAPI. However, the structure of certain dyes such as SYTOX Green, SYTO-9, and SYTO-24 remains undisclosed by the manufacturer, as this information is considered proprietary.

In the work [41], a novel approach utilizing GFP-labeled proteins as markers was introduced. This included RecA (DNA-repairing enzyme), DnaN (DNA polymerase subunit), RpoC (RNA polymerase subunit), and RpsB (ribosomal subunit) for visualization of main intracellular processes (DNA reparation, DNA replication, mRNA synthesis, protein synthesis, respectively). Genome-encoded fluorescent fusions are becoming a powerful tool for protein localization and mechanistic studies [36,42–46]. Subsequently, a chemical alternative to molecular biology-derived instruments was developed. Fluorescent-labelled wheat germ agglutinin was used for the detection of cell wall peptidoglycan [47,48] and a fluorescent-labelled anti-FtsZ antibody was used for a protein localization study [47]. However, these types of instruments are infrequently referenced in literature [35].

The utilization of test-strains is summarized on Fig. 4. The most frequently employed strains are *Escherichia coli* and *Bacillus subtilis*, because they are widely used as model organisms in bacteriology. Another reason is the high susceptibility (and resulting sensitivity) of these bacteria toward antibacterials. Despite *E. coli* being a gram-negative bacterium that is often resistant to many antibiotics, sensitized mutants bearing defects (*lptD4213* mutation) in cell wall porins (LptD) or deficient in the main protein in the efflux system (Δ*tolC*) are easily accessible and have wide susceptibility.

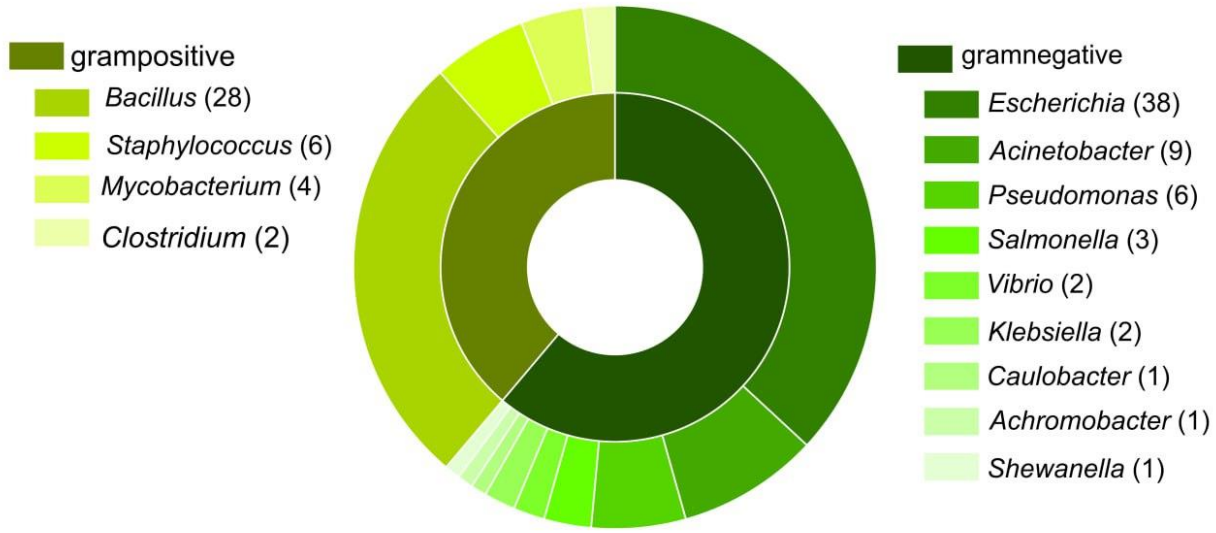

Fig. 4. Statistical analysis of test-strains usage

The first use of morphoprofilig for anaerobic bacteria (*Clostridium perfingens*) was described in [49]. Next year the methodology was expanded to include *Mycobacterium* species [50,51]. Anti-clostridial [52,53] and anti-mycobacterial [54,55] compounds represent a very specific chemical space and the successful application of phenotypic profiling in these cases indicates wide applicability of the imaging-based methods.

Conclusions and outlook

An in-depth examination of the bacterial phenotype – or bacterial phenomics – under the influence of antibiotics opens the path for the study of new effective ways to combat bacterial infections. Imaging-based profiling methods have emerged as valuable research tool for mechanistic studies of novel antibacterials as well as for investigation of combinations with conventional antibiotics and other therapeutic options. However, several challenges and limitations must be addressed to facilitate broader adoption of these approaches..

The small size of bacterial cells imposes many limitations on applicable imaging methods. A possible increase in the sensitivity and accuracy of profiling methods may be associated with the use of test cultures with larger cells (for example, *Bacillus megaterium*) or expansion microscopy approaches [56–58], making it possible to increase the resolution of the resulting images without noticeably complicating and increasing the cost of the experimental equipment used. Currently, confocal fluorescence microscopy stands as the predominant method for profiling purposes, yet employing simpler and more accessible optical microscopy techniques along with associated stains offers an appealing alternative.

The integration of automation methods for analyzing a large number of images, their segmentation, and machine learning algorithms for solving clustering and classification

problems opens up new opportunities for further successful use of morphoprofiling. At the moment, this option is rarely used in the reviewed works.

Funding

The work was supported by the Russian Science Foundation, project no. 22-74-00155, https://rscf.ru/en/project/22-74-00155/

Ethical statement

The authors declare no conflicts of interest. The funders had no role in the design of the study; in the collection, analyses, or interpretation of data; in the writing of the manuscript; or in the decision to publish the results.

Acknowledgments

We thank Mr. Alexander V. Korshun for technical help.

Abbreviations

ATCC – American Type Culture Collection, Me – methyl, Et – ethyl, Bu – buthyl, BCP – bacterial cytological profiling, MoA – mechanism of action, DBMI - dynamic bacterial morphology imaging.

References

1. Miethke, M.; Pieroni, M.; Weber, T.; Brönstrup, M.; Hammann, P.; Halby, L.; Arimondo, P.B.; Glaser, P.; Aigle, B.; Bode, H.B.; et al. Towards the Sustainable Discovery and Development of New Antibiotics. *Nat. Rev. Chem.* **2021**, *5*, 726–749, doi:10.1038/s41570-021-00313-1.
2. Baranova, A.A.; Alferova, V.A.; Korshun, V.A.; Tyurin, A.P. Modern Trends in Natural Antibiotic Discovery. *Life* **2023**, *13*, 1073, doi:10.3390/life13051073.
3. Hudson, M.A.; Lockless, S.W. Elucidating the Mechanisms of Action of Antimicrobial Agents. *mBio* **2022**, *13*, e02240-21, doi:10.1128/mbio.02240-21.
4. Cook, M.A.; Wright, G.D. The Past, Present, and Future of Antibiotics. *Sci. Transl. Med.* **2022**, *14*, eabo7793, doi:10.1126/scitranslmed.abo7793.
5. Lewis, K. The Science of Antibiotic Discovery. *Cell* **2020**, *181*, 29–45, doi:10.1016/j.cell.2020.02.056.
6. Baranova, A.A.; Tyurin, A.P.; Korshun, V.A.; Alferova, V.A. Sensing of Antibiotic–Bacteria Interactions. *Antibiotics* **2023**, *12*, 1340, doi:10.3390/antibiotics12081340.
7. Senges, C.H.R.; Stepanek, J.J.; Wenzel, M.; Raatschen, N.; Ay, Ü.; Märtens, Y.; Prochnow, P.; Vázquez Hernández, M.; Yayci, A.; Schubert, B.; et al. Comparison of Proteomic Responses as Global Approach to Antibiotic Mechanism of Action Elucidation. *Antimicrob. Agents Chemother.* **2020**, *65*, e01373-20, doi:10.1128/AAC.01373-20.
8. Ortmayr, K.; De La Cruz Moreno, R.; Zampieri, M. Expanding the Search for Small-Molecule Antibacterials by Multidimensional Profiling. *Nat. Chem. Biol.* **2022**, *18*, 584–595, doi:10.1038/s41589-022-01040-4.
9. Cotsonas King, A.; Wu, L. Macromolecular Synthesis and Membrane Perturbation Assays for Mechanisms of Action Studies of Antimicrobial Agents. *CP Pharmacology* **2009**, *47*, doi:10.1002/0471141755.ph13a07s47.
10. Cunningham, M.L.; Kwan, B.P.; Nelson, K.J.; Bensen, D.C.; Shaw, K.J. Distinguishing On-Target versus Off-Target Activity in Early Antibacterial Drug Discovery Using a Macromolecular Synthesis Assay. *SLAS Discovery* **2013**, *18*, 1018–1026, doi:10.1177/1087057113487208.
11. Farha, M.A.; Brown, E.D. Strategies for Target Identification of Antimicrobial Natural Products. *Nat. Prod. Rep.* **2016**, *33*, 668–680, doi:10.1039/c5np00127g.
12. Perlman, Z.E.; Slack, M.D.; Feng, Y.; Mitchison, T.J.; Wu, L.F.; Altschuler, S.J. Multidimensional Drug Profiling By Automated Microscopy. *Science* **2004**, *306*, 1194–1198, doi:10.1126/science.1100709.
13. Gardner, A.D. Morphological Effects of Penicillin on Bacteria. *Nature* **1940**, *146*, 837–838, doi:10.1038/146837b0.

14. Gardner, A. Microscopical effect of penicillin on spores and vegetative cells of bacilli. *The Lancet* **1945**, *245*, 658–659, doi:10.1016/S0140-6736(45)90043-2.
15. Duguid, J.P. The Sensitivity of Bacteria to the Action of Penicillin. *Edinb. Med. J.* **1946**, *53*, 401–412.
16. Ohya, Y.; Sese, J.; Yukawa, M.; Sano, F.; Nakatani, Y.; Saito, T.L.; Saka, A.; Fukuda, T.; Ishihara, S.; Oka, S.; et al. High-Dimensional and Large-Scale Phenotyping of Yeast Mutants. *Proc. Natl. Acad. Sci. U.S.A.* **2005**, *102*, 19015–19020, doi:10.1073/pnas.0509436102.
17. Ohnuki, S.; Oka, S.; Nogami, S.; Ohya, Y. High-Content, Image-Based Screening for Drug Targets in Yeast. *PLoS ONE* **2010**, *5*, e10177, doi:10.1371/journal.pone.0010177.
18. Lamsa, A.; Liu, W.; Dorrestein, P.C.; Pogliano, K. The *Bacillus Subtilis* Cannibalism Toxin SDP Collapses the Proton Motive Force and Induces Autolysis. *Mol. Microbiol.* **2012**, *84*, 486–500, doi:10.1111/j.1365-2958.2012.08038.x.
19. Nonejuie, P.; Burkart, M.; Pogliano, K.; Pogliano, J. Bacterial Cytological Profiling Rapidly Identifies the Cellular Pathways Targeted by Antibacterial Molecules. *Proc. Natl. Acad. Sci. U.S.A.* **2013**, *110*, 16169–16174, doi:10.1073/pnas.1311066110.
20. Ojkic, N.; Serbanescu, D.; Banerjee, S. Surface-to-Volume Scaling and Aspect Ratio Preservation in Rod-Shaped Bacteria. *eLife* **2019**, *8*, e47033, doi:10.7554/eLife.47033.
21. Ojkic, N.; Lilja, E.; Direito, S.; Dawson, A.; Allen, R.J.; Waclaw, B. A Roadblock-and-Kill Mechanism of Action Model for the DNA-Targeting Antibiotic Ciprofloxacin. *Antimicrob. Agents Chemother.* **2020**, *64*, e02487-19, doi:10.1128/AAC.02487-19.
22. Banerjee, S.; Lo, K.; Ojkic, N.; Stephens, R.; Scherer, N.F.; Dinner, A.R. Mechanical Feedback Promotes Bacterial Adaptation to Antibiotics. *Nat. Phys.* **2021**, *17*, 403–409, doi:10.1038/s41567-020-01079-x.
23. Serbanescu, D.; Ojkic, N.; Banerjee, S. Cellular Resource Allocation Strategies for Cell Size and Shape Control in Bacteria. *FEBS J.* **2022**, *289*, 7891–7906, doi:10.1111/febs.16234.
24. Ojkic, N.; Serbanescu, D.; Banerjee, S. Antibiotic Resistance via Bacterial Cell Shape-Shifting. *mBio* **2022**, *13*, e00659-22, doi:10.1128/mbio.00659-22.
25. Mack, S.G.; Turner, R.L.; Dwyer, D.J. Achieving a Predictive Understanding of Antimicrobial Stress Physiology through Systems Biology. *Trends Microbiol.* **2018**, *26*, 296–312, doi:10.1016/j.tim.2018.02.004.
26. Buck, A.K.; Elmore, D.E.; Darling, L.E. Using Fluorescence Microscopy to Shed Light on the Mechanisms of Antimicrobial Peptides. *Future Med. Chem.* **2019**, *11*, 2447–2460, doi:10.4155/fmc-2019-0095.
27. Ziegler, S.; Sievers, S.; Waldmann, H. Morphological Profiling of Small Molecules. *Cell Chem. Biol.* **2021**, *28*, 300–319, doi:10.1016/j.chembiol.2021.02.012.
28. Quach, D.T.; Sakoulas, G.; Nizet, V.; Pogliano, J.; Pogliano, K. Bacterial Cytological Profiling (BCP) as a Rapid and Accurate Antimicrobial Susceptibility Testing Method for Staphylococcus Aureus. *EBioMedicine* **2016**, *4*, 95–103, doi:10.1016/j.ebiom.2016.01.020.
29. Lamsa, A.; Lopez-Garrido, J.; Quach, D.; Riley, E.P.; Pogliano, J.; Pogliano, K. Rapid Inhibition Profiling in *Bacillus Subtilis* to Identify the Mechanism of Action of New Antimicrobials. *ACS Chem. Biol.* **2016**, *11*, 2222–2231, doi:10.1021/acschembio.5b01050.
30. Alexander, M.K.; Miu, A.; Oh, A.; Reichelt, M.; Ho, H.; Chalouni, C.; Labadie, S.; Wang, L.; Liang, J.; Nickerson, N.N.; et al. Disrupting Gram-Negative Bacterial Outer Membrane Biosynthesis through Inhibition of the Lipopolysaccharide Transporter MsbA. *Antimicrob. Agents Chemother.* **2018**, *62*, e01142-18, doi:10.1128/AAC.01142-18.
31. Sun, Y.; Heidary, D.K.; Zhang, Z.; Richards, C.I.; Glazer, E.C. Bacterial Cytological Profiling Reveals the Mechanism of Action of Anticancer Metal Complexes. *Mol. Pharmaceutics* **2018**, *15*, 3404–3416, doi:10.1021/acs.molpharmaceut.8b00407.
32. Coram, M.A.; Wang, L.; Godinez, W.J.; Barkan, D.T.; Armstrong, Z.; Ando, D.M.; Feng, B.Y. Morphological Characterization of Antibiotic Combinations. *ACS Infect. Dis.* **2022**, *8*, 66–77, doi:10.1021/acsinfecdis.1c00312.
33. Zoffmann, S.; Vercruysse, M.; Benmansour, F.; Maunz, A.; Wolf, L.; Blum Marti, R.; Heckel, T.; Ding, H.; Truong, H.H.; Prummer, M.; et al. Machine Learning-Powered Antibiotics Phenotypic Drug Discovery. *Sci. Rep.* **2019**, *9*, 5013, doi:10.1038/s41598-019-39387-9.

34. Sridhar, S.; Forrest, S.; Warne, B.; Maes, M.; Baker, S.; Dougan, G.; Bartholdson Scott, J. High-Content Imaging to Phenotype Antimicrobial Effects on Individual Bacteria at Scale. *mSystems* **2021**, *6*, e00028-21, doi:10.1128/mSystems.00028-21.
35. Sridhar, S.; Forrest, S.; Pickard, D.; Cormie, C.; Lees, E.A.; Thomson, N.R.; Dougan, G.; Baker, S. Inhibitory Concentrations of Ciprofloxacin Induce an Adaptive Response Promoting the Intracellular Survival of Salmonella Enterica Serovar Typhimurium. *mBio* **2021**, *12*, e01093-21, doi:10.1128/mBio.01093-21.
36. Mayer, B.; Schwan, M.; Thormann, K.M.; Graumann, P.L. Antibiotic Drug Screening and Image Characterization Toolbox (A.D.I.C.T.): A Robust Imaging Workflow to Monitor Antibiotic Stress Response in Bacterial Cells in Vivo. *F1000Res* **2021**, *10*, 277, doi:10.12688/f1000research.51868.1.
37. Krentzel, D.; Shorte, S.L.; Zimmer, C. Deep Learning in Image-Based Phenotypic Drug Discovery. *Trends Cell Biol.* **2023**, *33*, 538–554, doi:10.1016/j.tcb.2022.11.011.
38. Spahn, C.; Gómez-de-Mariscal, E.; Laine, R.F.; Pereira, P.M.; Von Chamier, L.; Conduit, M.; Pinho, M.G.; Jacquemet, G.; Holden, S.; Heilemann, M.; et al. DeepBacs for Multi-Task Bacterial Image Analysis Using Open-Source Deep Learning Approaches. *Commun. Biol.* **2022**, *5*, 688, doi:10.1038/s42003-022-03634-z.
39. Ouyang, X.; Hoeksma, J.; Lubbers, R.J.M.; Siersma, T.K.; Hamoen, L.W.; Den Hertog, J. Classification of Antimicrobial Mechanism of Action Using Dynamic Bacterial Morphology Imaging. *Sci. Rep.* **2022**, *12*, 11162, doi:10.1038/s41598-022-15405-1.
40. Ouyang, X.; Hoeksma, J.; Beenker, W.A.G.; Van Der Beek, S.; Den Hertog, J. Harzianic Acid Exerts Antimicrobial Activity against Gram-Positive Bacteria and Targets the Cell Membrane. *Front. Microbiol.* **2024**, *15*, 1332774, doi:10.3389/fmicb.2024.1332774.
41. Saeloh, D.; Tipmanee, V.; Jim, K.K.; Dekker, M.P.; Bitter, W.; Voravuthikunchai, S.P.; Wenzel, M.; Hamoen, L.W. The Novel Antibiotic Rhodomyrtone Traps Membrane Proteins in Vesicles with Increased Fluidity. *PLoS Pathog.* **2018**, *14*, e1006876, doi:10.1371/journal.ppat.1006876.
42. Kamal El-sagheir, A.M.; Abdelmesseh Nekhala, I.; Abd El-Gaber, M.K.; Aboraia, A.S.; Persson, J.; Schäfer, A.-B.; Wenzel, M.; Omar, F.A. Design, Synthesis, Molecular Modeling, Biological Activity, and Mechanism of Action of Novel Amino Acid Derivatives of Norfloxacin. *ACS Omega* **2023**, *8*, 43271–43284, doi:10.1021/acsomega.3c07221.
43. Kamal El-sagheir, A.M.; Abdelmesseh Nekhala, I.; Abd El-Gaber, M.K.; Aboraia, A.S.; Persson, J.; Schäfer, A.-B.; Wenzel, M.; Omar, F.A. N4-Substituted Piperazinyl Norfloxacin Derivatives with Broad-Spectrum Activity and Multiple Mechanisms on Gyrase, Topoisomerase IV, and Bacterial Cell Wall Synthesis. *ACS Bio Med Chem Au* **2023**, *3*, 494–506, doi:10.1021/acsbiomedchemau.3c00038.
44. Kepplinger, B.; Mardiana, L.; Cowell, J.; Morton-Laing, S.; Dashti, Y.; Wills, C.; Marrs, E.C.L.; Perry, J.D.; Gray, J.; Goodfellow, M.; et al. Discovery, Isolation, Heterologous Expression and Mode-of-Action Studies of the Antibiotic Polyketide Tatiomicin from Amycolatopsis Sp. DEM30355. *Sci. Rep.* **2022**, *12*, 15579, doi:10.1038/s41598-022-18726-3.
45. Andreu, J.M.; Huecas, S.; Araújo-Bazán, L.; Vázquez-Villa, H.; Martín-Fontecha, M. The Search for Antibacterial Inhibitors Targeting Cell Division Protein FtsZ at Its Nucleotide and Allosteric Binding Sites. *Biomedicines* **2022**, *10*, 1825, doi:10.3390/biomedicines10081825.
46. Kamal El-sagheir, A.M.; Abdelmesseh Nekhala, I.; Abd El-Gaber, M.K.; Aboraia, A.S.; Persson, J.; Schäfer, A.-B.; Wenzel, M.; Omar, F.A. Rational Design, Synthesis, Molecular Modeling, Biological Activity, and Mechanism of Action of Polypharmacological Norfloxacin Hydroxamic Acid Derivatives. *RSC Med. Chem.* **2023**, *14*, 2593–2610, doi:10.1039/D3MD00309D.
47. McAuley, S.; Vadia, S.; Jani, C.; Huynh, A.; Yang, Z.; Levin, P.A.; Nodwell, J.R. A Chemical Inhibitor of Cell Growth Reduces Cell Size in *Bacillus Subtilis*. *ACS Chem. Biol.* **2019**, *14*, 688–695, doi:10.1021/acschembio.8b01066.
48. Cauz, A.C.G.; Carretero, G.P.B.; Saraiva, G.K.V.; Park, P.; Mortara, L.; Cuccovia, I.M.; Brocchi, M.; Gueiros-Filho, F.J. Violacein Targets the Cytoplasmic Membrane of Bacteria. *ACS Infect. Dis.* **2019**, *5*, 539–549, doi:10.1021/acsinfecdis.8b00245.
49. Chiumento, S.; Roblin, C.; Kieffer-Jaquinod, S.; Tachon, S.; Leprètre, C.; Basset, C.; Aditiyarini, D.; Olleik, H.; Nicoletti, C.; Bornet, O.; et al. Ruminococcin C, a Promising Antibiotic Produced by a Human Gut Symbiont. *Sci. Adv.* **2019**, *5*, eaaw9969, doi:10.1126/sciadv.aaw9969.
50. De Wet, T.J.; Winkler, K.R.; Mhlanga, M.; Mizrahi, V.; Warner, D.F. Arrayed CRISPRi and Quantitative Imaging Describe the Morphotypic Landscape of Essential Mycobacterial Genes. *eLife* **2020**, *9*, e60083, doi:10.7554/eLife.60083.

51. Smith, T.C.; Pullen, K.M.; Olson, M.C.; McNellis, M.E.; Richardson, I.; Hu, S.; Larkins-Ford, J.; Wang, X.; Freundlich, J.S.; Ando, D.M.; et al. Morphological Profiling of Tubercle Bacilli Identifies Drug Pathways of Action. *Proc. Natl. Acad. Sci. U.S.A.* **2020**, *117*, 18744–18753, doi:10.1073/pnas.2002738117.
52. Alshrari, A.S.; Hudu, S.A.; Elmigdadi, F.; Imran, Mohd. The Urgent Threat of Clostridioides Difficile Infection: A Glimpse of the Drugs of the Future, with Related Patents and Prospects. *Biomedicines* **2023**, *11*, 426, doi:10.3390/biomedicines11020426.
53. Carlson, T.J.; Gonzales-Luna, A.J. Antibiotic Treatment Pipeline for Clostridioides Difficile Infection (CDI): A Wide Array of Narrow-Spectrum Agents. *Curr. Infect. Dis. Rep.* **2020**, *22*, 20, doi:10.1007/s11908-020-00730-1.
54. Campaniço, A.; Moreira, R.; Lopes, F. Drug Discovery in Tuberculosis. New Drug Targets and Antimycobacterial Agents. *Eur. J. Med. Chem.* **2018**, *150*, 525–545, doi:10.1016/j.ejmech.2018.03.020.
55. Han, J.; Liu, X.; Zhang, L.; Quinn, R.J.; Feng, Y. Anti-Mycobacterial Natural Products and Mechanisms of Action. *Nat. Prod. Rep.* **2022**, *39*, 77–89, doi:10.1039/D1NP00011J.
56. Carsten, A.; Wolters, M.; Aepfelbacher, M. Super-resolution Fluorescence Microscopy for Investigating Bacterial Cell Biology. *Mol. Microbiol.* **2024**, *121*, 646–658, doi:10.1111/mmi.15203.
57. Zhuang, Y.; Shi, X. Expansion Microscopy: A Chemical Approach for Super-Resolution Microscopy. *Curr. Opin. Struct. Biol.* **2023**, *81*, 102614, doi:10.1016/j.sbi.2023.102614.
58. Truckenbrodt, S. Expansion Microscopy: Super-Resolution Imaging with Hydrogels. *Anal. Chem.* **2023**, *95*, 3–32, doi:10.1021/acs.analchem.2c04921.
59. Jayamani, E.; Rajamuthiah, R.; Larkins-Ford, J.; Fuchs, B.B.; Conery, A.L.; Vilcinskas, A.; Ausubel, F.M.; Mylonakis, E. Insect-Derived Cecropins Display Activity against *Acinetobacter Baumannii* in a Whole-Animal High-Throughput Caenorhabditis Elegans Model. *Antimicrob. Agents. Chemother.* **2015**, *59*, 1728–1737, doi:10.1128/AAC.04198-14.
60. Artola, M.; Ruiz-Avila, L.B.; Vergoñós, A.; Huecas, S.; Araujo-Bazán, L.; Martín-Fontecha, M.; Vázquez-Villa, H.; Turrado, C.; Ramírez-Aportela, E.; Hoegl, A.; et al. Effective GTP-Replacing FtsZ Inhibitors and Antibacterial Mechanism of Action. *ACS Chem. Biol.* **2015**, *10*, 834–843, doi:10.1021/cb500974d.
61. Lin, L.; Nonejuie, P.; Munguia, J.; Hollands, A.; Olson, J.; Dam, Q.; Kumaraswamy, M.; Rivera, H.; Corriden, R.; Rohde, M.; et al. Azithromycin Synergizes with Cationic Antimicrobial Peptides to Exert Bactericidal and Therapeutic Activity Against Highly Multidrug-Resistant Gram-Negative Bacterial Pathogens. *EBioMedicine* **2015**, *2*, 690–698, doi:10.1016/j.ebiom.2015.05.021.
62. McLeod, S.M.; Fleming, P.R.; MacCormack, K.; McLaughlin, R.E.; Whiteaker, J.D.; Narita, S.; Mori, M.; Tokuda, H.; Miller, A.A. Small-Molecule Inhibitors of Gram-Negative Lipoprotein Trafficking Discovered by Phenotypic Screening. *J. Bacteriol.* **2015**, *197*, 1075–1082, doi:10.1128/JB.02352-14.
63. Nayar, A.S.; Dougherty, T.J.; Ferguson, K.E.; Granger, B.A.; McWilliams, L.; Stacey, C.; Leach, L.J.; Narita, S.; Tokuda, H.; Miller, A.A.; et al. Novel Antibacterial Targets and Compounds Revealed by a High-Throughput Cell Wall Reporter Assay. *J. Bacteriol.* **2015**, *197*, 1726–1734, doi:10.1128/JB.02552-14.
64. Araújo-Bazán, L.; Ruiz-Avila, L.B.; Andreu, D.; Huecas, S.; Andreu, J.M. Cytological Profile of Antibacterial FtsZ Inhibitors and Synthetic Peptide MciZ. *Front. Microbiol.* **2016**, *7*, doi:10.3389/fmicb.2016.01558.
65. Nonejuie, P.; Trial, R.M.; Newton, G.L.; Lamsa, A.; Ranmali Perera, V.; Aguilar, J.; Liu, W.-T.; Dorrestein, P.C.; Pogliano, J.; Pogliano, K. Application of Bacterial Cytological Profiling to Crude Natural Product Extracts Reveals the Antibacterial Arsenal of Bacillus Subtilis. *J Antibiot* **2016**, *69*, 353–361, doi:10.1038/ja.2015.116.
66. Wang, M.; Carver, J.J.; Phelan, V.V.; Sanchez, L.M.; Garg, N.; Peng, Y.; Nguyen, D.D.; Watrous, J.; Kapono, C.A.; Luzzatto-Knaan, T.; et al. Sharing and Community Curation of Mass Spectrometry Data with Global Natural Products Social Molecular Networking. *Nat. Biotechnol.* **2016**, *34*, 828–837, doi:10.1038/nbt.3597.
67. Wilson, M.Z.; Wang, R.; Gitai, Z.; Seyedsayamdost, M.R. Mode of Action and Resistance Studies Unveil New Roles for Tropodithietic Acid as an Anticancer Agent and the γ-Glutamyl Cycle as a Proton Sink. *Proc. Natl. Acad. Sci. U.S.A.* **2016**, *113*, 1630–1635, doi:10.1073/pnas.1518034113.

68. Wu, Y.; Seyedsayamdost, M.R. Synergy and Target Promiscuity Drive Structural Divergence in Bacterial Alkylquinolone Biosynthesis. *Cell Chem. Biol.* **2017**, *24*, 1437-1444.e3, doi:10.1016/j.chembiol.2017.08.024.
69. Eid, I.; Elsebaei, M.M.; Mohammad, H.; Hagras, M.; Peters, C.E.; Hegazy, Y.A.; Cooper, B.; Pogliano, J.; Pogliano, K.; Abulkhair, H.S.; et al. Arylthiazole Antibiotics Targeting Intracellular Methicillin-Resistant *Staphylococcus Aureus* (MRSA) That Interfere with Bacterial Cell Wall Synthesis. *Eur. J. Med. Chem.* **2017**, *139*, 665–673, doi:10.1016/j.ejmech.2017.08.039.
70. Mohammad, H.; Younis, W.; Chen, L.; Peters, C.E.; Pogliano, J.; Pogliano, K.; Cooper, B.; Zhang, J.; Mayhoub, A.; Oldfield, E.; et al. Phenylthiazole Antibacterial Agents Targeting Cell Wall Synthesis Exhibit Potent Activity in Vitro and in Vivo against Vancomycin-Resistant Enterococci. *J. Med. Chem.* **2017**, *60*, 2425–2438, doi:10.1021/acs.jmedchem.6b01780.
71. Durand-Réville, T.F.; Guler, S.; Comita-Prevoir, J.; Chen, B.; Bifulco, N.; Huynh, H.; Lahiri, S.; Shapiro, A.B.; McLeod, S.M.; Carter, N.M.; et al. ETX2514 Is a Broad-Spectrum β-Lactamase Inhibitor for the Treatment of Drug-Resistant Gram-Negative Bacteria Including Acinetobacter Baumannii. *Nat. Microbiol.* **2017**, *2*, 17104, doi:10.1038/nmicrobiol.2017.104.
72. Sarkar, P.; Switzer, A.; Peters, C.; Pogliano, J.; Wigneshweraraj, S. Phenotypic Consequences of RNA Polymerase Dysregulation in Escherichia Coli. *Nucleic Acids Res.* **2017**, *45*, 11131–11143, doi:10.1093/nar/gkx733.
73. Mohammad, H.; Younis, W.; Ezzat, H.G.; Peters, C.E.; AbdelKhalek, A.; Cooper, B.; Pogliano, K.; Pogliano, J.; Mayhoub, A.S.; Seleem, M.N. Bacteriological Profiling of Diphenylureas as a Novel Class of Antibiotics against Methicillin-Resistant *Staphylococcus Aureus*. *PLoS ONE* **2017**, *12*, e0182821, doi:10.1371/journal.pone.0182821.
74. Santos, T.M.A.; Lammers, M.G.; Zhou, M.; Sparks, I.L.; Rajendran, M.; Fang, D.; De Jesus, C.L.Y.; Carneiro, G.F.R.; Cui, Q.; Weibel, D.B. Small Molecule Chelators Reveal That Iron Starvation Inhibits Late Stages of Bacterial Cytokinesis. *ACS Chem. Biol.* **2018**, *13*, 235–246, doi:10.1021/acschembio.7b00560.
75. Peters, C.E.; Lamsa, A.; Liu, R.B.; Quach, D.; Sugie, J.; Brumage, L.; Pogliano, J.; Lopez-Garrido, J.; Pogliano, K. Rapid Inhibition Profiling Identifies a Keystone Target in the Nucleotide Biosynthesis Pathway. *ACS Chem. Biol.* **2018**, *13*, 3251–3258, doi:10.1021/acschembio.8b00273.
76. Dean, C.R.; Barkan, D.T.; Bermingham, A.; Blais, J.; Casey, F.; Casarez, A.; Colvin, R.; Fuller, J.; Jones, A.K.; Li, C.; et al. Mode of Action of the Monobactam LYS228 and Mechanisms Decreasing *In Vitro* Susceptibility in *Escherichia Coli* and *Klebsiella Pneumoniae*. *Antimicrob. Agents Chemother.* **2018**, *62*, e01200-18, doi:10.1128/AAC.01200-18.
77. Wu, Y.; Seyedsayamdost, M.R. The Polyene Natural Product Thailandamide A Inhibits Fatty Acid Biosynthesis in Gram-Positive and Gram-Negative Bacteria. *Biochemistry* **2018**, *57*, 4247–4251, doi:10.1021/acs.biochem.8b00678.
78. Liu, C.; Qi, J.; Shan, B.; Ma, Y. Tachyplesin Causes Membrane Instability That Kills Multidrug-Resistant Bacteria by Inhibiting the 3-Ketoacyl Carrier Protein Reductase FabG. *Front. Microbiol.* **2018**, *9*, 825, doi:10.3389/fmicb.2018.00825.
79. Gupta, N.; Liu, R.; Shin, S.; Sinha, R.; Pogliano, J.; Pogliano, K.; Griffin, J.H.; Nizet, V.; Corriden, R. SCH79797 Improves Outcomes in Experimental Bacterial Pneumonia by Boosting Neutrophil Killing and Direct Antibiotic Activity. *J. Antimicrob. Chemother.* **2018**, *73*, 1586–1594, doi:10.1093/jac/dky033.
80. Deblais, L.; Helmy, Y.A.; Kathayat, D.; Huang, H.; Miller, S.A.; Rajashekara, G. Novel Imidazole and Methoxybenzylamine Growth Inhibitors Affecting Salmonella Cell Envelope Integrity and Its Persistence in Chickens. *Sci. Rep.* **2018**, *8*, 13381, doi:10.1038/s41598-018-31249-0.
81. Kathayat, D.; Helmy, Y.A.; Deblais, L.; Rajashekara, G. Novel Small Molecules Affecting Cell Membrane as Potential Therapeutics for Avian Pathogenic *Escherichia Coli*. *Sci. Rep.* **2018**, *8*, 15329, doi:10.1038/s41598-018-33587-5.
82. Godinez, W.J.; Chan, H.; Hossain, I.; Li, C.; Ranjitkar, S.; Rasper, D.; Simmons, R.L.; Zhang, X.; Feng, B.Y. Morphological Deconvolution of Beta-Lactam Polyspecificity in *E. Coli*. *ACS Chem. Biol.* **2019**, *14*, 1217–1226, doi:10.1021/acschembio.9b00141.
83. Htoo, H.H.; Brumage, L.; Chaikeeratisak, V.; Tsunemoto, H.; Sugie, J.; Tribuddharat, C.; Pogliano, J.; Nonejuie, P. Bacterial Cytological Profiling as a Tool To Study Mechanisms of Action of Antibiotics That Are Active against Acinetobacter Baumannii. *Antimicrob. Agents Chemother.* **2019**, *63*, e02310-18, doi:10.1128/AAC.02310-18.

84. Dillon, N.; Holland, M.; Tsunemoto, H.; Hancock, B.; Cornax, I.; Pogliano, J.; Sakoulas, G.; Nizet, V. Surprising Synergy of Dual Translation Inhibition vs. *Acinetobacter Baumannii* and Other Multidrug-Resistant Bacterial Pathogens. *eBioMedicine* **2019**, *46*, 193–201, doi:10.1016/j.ebiom.2019.07.041.
85. Andrews, L.D.; Kane, T.R.; Dozzo, P.; Haglund, C.M.; Hilderbrandt, D.J.; Linsell, M.S.; Machajewski, T.; McEnroe, G.; Serio, A.W.; Wlasichuk, K.B.; et al. Optimization and Mechanistic Characterization of Pyridopyrimidine Inhibitors of Bacterial Biotin Carboxylase. *J. Med. Chem.* **2019**, *62*, 7489–7505, doi:10.1021/acs.jmedchem.9b00625.
86. Rajput, A.; Poudel, S.; Tsunemoto, H.; Meehan, M.; Szubin, R.; Olson, C.A.; Lamsa, A.; Seif, Y.; Dillon, N.; Vrbanac, A.; et al. Profiling the Effect of Nafcillin on HA-MRSA D712 Using Bacteriological and Physiological Media. *Sci. Data* **2019**, *6*, 322, doi:10.1038/s41597-019-0331-z.
87. Chamberlin, J.; Story, S.; Ranjan, N.; Chesser, G.; Arya, D.P. Gram-Negative Synergy and Mechanism of Action of Alkynyl Bisbenzimidazoles. *Sci. Rep.* **2019**, *9*, 14171, doi:10.1038/s41598-019-48898-4.
88. Olleik, H.; Nicoletti, C.; Lafond, M.; Courvoisier-Dezord, E.; Xue, P.; Hijazi, A.; Baydoun, E.; Perrier, J.; Maresca, M. Comparative Structure–Activity Analysis of the Antimicrobial Activity, Cytotoxicity, and Mechanism of Action of the Fungal Cyclohexadepsipeptides Enniatins and Beauvericin. *Toxins* **2019**, *11*, 514, doi:10.3390/toxins11090514.
89. Juliano, S.A.; Serafim, L.F.; Duay, S.S.; Heredia Chavez, M.; Sharma, G.; Rooney, M.; Comert, F.; Pierce, S.; Radulescu, A.; Cotten, M.L.; et al. A Potent Host Defense Peptide Triggers DNA Damage and Is Active against Multidrug-Resistant Gram-Negative Pathogens. *ACS Infect. Dis.* **2020**, *6*, 1250–1263, doi:10.1021/acsinfecdis.0c00051.
90. Miller, A.A.; Shapiro, A.B.; McLeod, S.M.; Carter, N.M.; Moussa, S.H.; Tommasi, R.; Mueller, J.P. *In Vitro* Characterization of ETX1317, a Broad-Spectrum β-Lactamase Inhibitor That Restores and Enhances β-Lactam Activity against Multi-Drug-Resistant *Enterobacteriales* , Including Carbapenem-Resistant Strains. *ACS Infect. Dis.* **2020**, *6*, 1389–1397, doi:10.1021/acsinfecdis.0c00020.
91. Martin, J.K.; Sheehan, J.P.; Bratton, B.P.; Moore, G.M.; Mateus, A.; Li, S.H.-J.; Kim, H.; Rabinowitz, J.D.; Typas, A.; Savitski, M.M.; et al. A Dual-Mechanism Antibiotic Kills Gram-Negative Bacteria and Avoids Drug Resistance. *Cell* **2020**, *181*, 1518-1532.e14, doi:10.1016/j.cell.2020.05.005.
92. Coulibaly, S.; Cimino, M.; Ouattara, M.; Lecoutey, C.; Buchieri, M.V.; Alonso-Rodriguez, N.; Briffotaux, J.; Mornico, D.; Gicquel, B.; Rochais, C.; et al. Phenanthrolinic Analogs of Quinolones Show Antibacterial Activity against M. Tuberculosis. *Eur. J. Med. Chem.* **2020**, *207*, 112821, doi:10.1016/j.ejmech.2020.112821.
93. Ulloa, E.R.; Kousha, A.; Tsunemoto, H.; Pogliano, J.; Licitra, C.; LiPuma, J.J.; Sakoulas, G.; Nizet, V.; Kumaraswamy, M. Azithromycin Exerts Bactericidal Activity and Enhances Innate Immune Mediated Killing of MDR Achromobacter Xylosoxidans. *Infect. Microbes Dis .* **2020**, *2*, 10–17, doi:10.1097/IM9.0000000000000014.
94. Bhando, T.; Bhattacharyya, T.; Gaurav, A.; Akhter, J.; Saini, M.; Gupta, V.K.; Srivastava, S.K.; Sen, H.; Navani, N.K.; Gupta, V.; et al. Antibacterial Properties and in Vivo Efficacy of a Novel Nitrofuran, IITR06144, against MDR Pathogens. *J. Antimicrob. Chemother.* **2019**, dkz428, doi:10.1093/jac/dkz428.
95. Thammatinna, K.; Egan, M.E.; Htoo, H.H.; Khanna, K.; Sugie, J.; Nideffer, J.F.; Villa, E.; Tassanakajon, A.; Pogliano, J.; Nonejuie, P.; et al. A Novel Vibriophage Exhibits Inhibitory Activity against Host Protein Synthesis Machinery. *Sci. Rep.* **2020**, *10*, 2347, doi:10.1038/s41598-020-59396-3.
96. Tyurin, A.P.; Alferova, V.A.; Paramonov, A.S.; Shuvalov, M.V.; Kudryakova, G.K.; Rogozhin, E.A.; Zherebker, A.Y.; Brylev, V.A.; Chistov, A.A.; Baranova, A.A.; et al. Gausemycins A,B: Cyclic Lipoglycopeptides from *Streptomyces* Sp.**. *Angew. Chem. Int. Ed.* **2021**, *60*, 18694–18703, doi:10.1002/anie.202104528.
97. Kathayat, D.; Closs, G.; Helmy, Y.A.; Lokesh, D.; Ranjit, S.; Rajashekara, G. Peptides Affecting the Outer Membrane Lipid Asymmetry System (MlaA-OmpC/F) Reduce Avian Pathogenic Escherichia Coli (APEC) Colonization in Chickens. *Appl. Environ. Microbiol.* **2021**, *87*, e00567-21, doi:10.1128/AEM.00567-21.

98. Blaskovich, M.A.T.; Kavanagh, A.M.; Elliott, A.G.; Zhang, B.; Ramu, S.; Amado, M.; Lowe, G.J.; Hinton, A.O.; Pham, D.M.T.; Zuegg, J.; et al. The Antimicrobial Potential of Cannabidiol. *Commun. Biol.* **2021**, *4*, 7, doi:10.1038/s42003-020-01530-y.
99. O'Neill, A.M.; Worthing, K.A.; Kulkarni, N.; Li, F.; Nakatsuji, T.; McGrosso, D.; Mills, R.H.; Kalla, G.; Cheng, J.Y.; Norris, J.M.; et al. Antimicrobials from a Feline Commensal Bacterium Inhibit Skin Infection by Drug-Resistant S. Pseudintermedius. *eLife* **2021**, *10*, e66793, doi:10.7554/eLife.66793.
100. Rajput, A.; Poudel, S.; Tsunemoto, H.; Meehan, M.; Szubin, R.; Olson, C.A.; Seif, Y.; Lamsa, A.; Dillon, N.; Vrbanac, A.; et al. Identifying the Effect of Vancomycin on Health Care–Associated Methicillin-Resistant *Staphylococcus Aureus* Strains Using Bacteriological and Physiological Media. *GigaScience* **2021**, *10*, giaa156, doi:10.1093/gigascience/giaa156.
101. Montaño, E.T.; Nideffer, J.F.; Sugie, J.; Enustun, E.; Shapiro, A.B.; Tsunemoto, H.; Derman, A.I.; Pogliano, K.; Pogliano, J. Bacterial Cytological Profiling Identifies Rhodanine-Containing PAINS Analogs as Specific Inhibitors of *Escherichia Coli* Thymidylate Kinase *In Vivo*. *J. Bacteriol.* **2021**, *203*, doi:10.1128/JB.00105-21.
102. Pierce, E.C.; Morin, M.; Little, J.C.; Liu, R.B.; Tannous, J.; Keller, N.P.; Pogliano, K.; Wolfe, B.E.; Sanchez, L.M.; Dutton, R.J. Bacterial–Fungal Interactions Revealed by Genome-Wide Analysis of Bacterial Mutant Fitness. *Nat. Microbiol.* **2020**, *6*, 87–102, doi:10.1038/s41564-020-00800-z.
103. Durand-Reville, T.F.; Miller, A.A.; O'Donnell, J.P.; Wu, X.; Sylvester, M.A.; Guler, S.; Iyer, R.; Shapiro, A.B.; Carter, N.M.; Velez-Vega, C.; et al. Rational Design of a New Antibiotic Class for Drug-Resistant Infections. *Nature* **2021**, *597*, 698–702, doi:10.1038/s41586-021-03899-0.
104. Zhang, L.; Esquembre, L.A.; Xia, S.-N.; Oesterhelt, F.; Hughes, C.C.; Brötz-Oesterhelt, H.; Teufel, R. Antibacterial Synnepyrroles from Human-Associated *Nocardiopsis* Sp. Show Protonophore Activity and Disrupt the Bacterial Cytoplasmic Membrane. *ACS Chem. Biol.* **2022**, *17*, 2836–2848, doi:10.1021/acschembio.2c00460.
105. Menon, N.D.; Penziner, S.; Montaño, E.T.; Zurich, R.; Pride, D.T.; Nair, B.G.; Kumar, G.B.; Nizet, V. Increased Innate Immune Susceptibility in Hyperpigmented Bacteriophage-Resistant Mutants of Pseudomonas Aeruginosa. *Antimicrob. Agents Chemother.* **2022**, *66*, e00239-22, doi:10.1128/aac.00239-22.
106. Sun, D.; Tsivkovski, R.; Pogliano, J.; Tsunemoto, H.; Nelson, K.; Rubio-Aparicio, D.; Lomovskaya, O. Intrinsic Antibacterial Activity of Xeruborbactam *In Vitro* : Assessing Spectrum and Mode of Action. *Antimicrob. Agents Chemother.* **2022**, *66*, e00879-22, doi:10.1128/aac.00879-22.
107. Khan, N.A.; Kaur, N.; Owens, P.; Thomas, O.P.; Boyd, A. Bis-Indole Alkaloids Isolated from the Sponge Spongosorites Calcicola Disrupt Cell Membranes of MRSA. *IJMS* **2022**, *23*, 1991, doi:10.3390/ijms23041991.
108. Podoll, J.D.; Rosen, E.; Wang, W.; Gao, Y.; Zhang, J.; Wang, X. A Small-Molecule Membrane Fluidizer Re-Sensitizes Methicillin-Resistant *Staphylococcus Aureus* (MRSA) to β-Lactam Antibiotics. *Antimicrob. Agents Chemother.* **2023**, *67*, e00051-23, doi:10.1128/aac.00051-23.
109. Imai, Y.; Hauk, G.; Quigley, J.; Liang, L.; Son, S.; Ghiglieri, M.; Gates, M.F.; Morrissette, M.; Shahsavari, N.; Niles, S.; et al. Evybactin Is a DNA Gyrase Inhibitor That Selectively Kills Mycobacterium Tuberculosis. *Nat. Chem. Biol.* **2022**, *18*, 1236–1244, doi:10.1038/s41589-022-01102-7.
110. Rajput, A.; Tsunemoto, H.; Sastry, A.V.; Szubin, R.; Rychel, K.; Chauhan, S.M.; Pogliano, J.; Palsson, B.O. Advanced Transcriptomic Analysis Reveals the Role of Efflux Pumps and Media Composition in Antibiotic Responses of *Pseudomonas Aeruginosa*. *Nucleic Acids Res.* **2022**, *50*, 9675–9688, doi:10.1093/nar/gkac743.
111. Montaño, E.T.; Nideffer, J.F.; Brumage, L.; Erb, M.; Busch, J.; Fernandez, L.; Derman, A.I.; Davis, J.P.; Estrada, E.; Fu, S.; et al. Isolation and Characterization of Streptomyces Bacteriophages and Streptomyces Strains Encoding Biosynthetic Arsenals. *PLoS ONE* **2022**, *17*, e0262354, doi:10.1371/journal.pone.0262354.
112. Htoo, H.H.; Tuyet, N.N.T.; Nakprasit, K.; Aonbangkhen, C.; Chaikeeratisak, V.; Chavasiri, W.; Nonejuie, P. Mansonone G and Its Derivatives Exhibit Membrane Permeabilizing Activities against Bacteria. *PLoS ONE* **2022**, *17*, e0273614, doi:10.1371/journal.pone.0273614.
113. Herschede, S.R.; Salam, R.; Gneid, H.; Busschaert, N. Bacterial Cytological Profiling Identifies Transmembrane Anion Transport as the Mechanism of Action for a Urea-Based Antibiotic. *Supramol. Chem.* **2022**, *34*, 26–33, doi:10.1080/10610278.2023.2178921.

114. Soonthonsrima, T.; Htoo, H.H.; Thiennimitr, P.; Srisuknimit, V.; Nonejuie, P.; Chaikeeratisak, V. Phage-Induced Bacterial Morphological Changes Reveal a Phage-Derived Antimicrobial Affecting Cell Wall Integrity. *Antimicrob. Agents Chemother.* **2023**, *67*, e00764-23, doi:10.1128/aac.00764-23.
115. He, Q.; Yang, Z.; Zou, Z.; Qian, M.; Wang, X.; Zhang, X.; Yin, Z.; Wang, J.; Ye, X.; Liu, D.; et al. Combating *Escherichia Coli* O157:H7 with Functionalized Chickpea-Derived Antimicrobial Peptides. *Adv. Sci.* **2023**, *10*, 2205301, doi:10.1002/advs.202205301.
116. Samernate, T.; Htoo, H.H.; Sugie, J.; Chavasiri, W.; Pogliano, J.; Chaikeeratisak, V.; Nonejuie, P. High-Resolution Bacterial Cytological Profiling Reveals Intrapopulation Morphological Variations upon Antibiotic Exposure. *Antimicrob. Agents Chemother.* **2023**, *67*, e01307-22, doi:10.1128/aac.01307-22.
117. Upender, I.; Yoshida, O.; Schrecengost, A.; Ranson, H.; Wu, Q.; Rowley, D.C.; Kishore, S.; Cywes, C.; Miller, E.L.; Whalen, K.E. A Marine-Derived Fatty Acid Targets the Cell Membrane of Gram-Positive Bacteria. *J. Bacteriol.* **2023**, *205*, e00310-23, doi:10.1128/jb.00310-23.
118. Zhang, Y.; Kepiro, I.; Ryadnov, M.G.; Pagliara, S. Single Cell Killing Kinetics Differentiate Phenotypic Bacterial Responses to Different Antibacterial Classes. *Microbiol. Spectr.* **2023**, *11*, e03667-22, doi:10.1128/spectrum.03667-22.
119. Tsunemoto, H.; Sugie, J.; Enustun, E.; Pogliano, K.; Pogliano, J. Bacterial Cytological Profiling Reveals Interactions between Jumbo Phage φKZ Infection and Cell Wall Active Antibiotics in Pseudomonas Aeruginosa. *PLoS ONE* **2023**, *18*, e0280070, doi:10.1371/journal.pone.0280070.
120. Beyer, L.I.; Schäfer, A.-B.; Undabarrena, A.; Mattsby-Baltzer, I.; Tietze, D.; Svensson, E.; Stubelius, A.; Wenzel, M.; Cámara, B.; Tietze, A.A. Mimicking Nonribosomal Peptides from the Marine Actinomycete *Streptomyces* Sp. H-KF8 Leads to Antimicrobial Peptides. *ACS Infect. Dis.* **2024**, *10*, 79–92, doi:10.1021/acsinfecdis.3c00206.
121. Scaccaglia, M.; Birbaumer, M.P.; Pinelli, S.; Pelosi, G.; Frei, A. Discovery of Antibacterial Manganese(I) Tricarbonyl Complexes through Combinatorial Chemistry. *Chem. Sci.* **2024**, *15*, 3907–3919, doi:10.1039/D3SC05326A.
122. Schäfer, A.-B.; Sidarta, M.; Abdelmesseh Nekhala, I.; Marinho Righetto, G.; Arshad, A.; Wenzel, M. Dissecting Antibiotic Effects on the Cell Envelope Using Bacterial Cytological Profiling: A Phenotypic Analysis Starter Kit. *Microbiol. Spectr.* **2024**, *12*, e03275-23, doi:10.1128/spectrum.03275-23.

Appendix A. Selected publications

Year	Ref.	Base method (ref.)	Dyes, probes	Test culture	Object of study	Main results
2012	[18]	-	FM4–64, SYTOXGreen, DAPI	*Bacillus subtilis* (different strains)	*Bacillus subtilis* SDP peptide toxin	Using cytoprofiling, it was shown that the effect of SDP toxin is close to the effect of dinitrophenol, azide and CCCP.
2013	[19]	-	FM4–64, SYTOXGreen, DAPI	*Escherichia coli lptD4213*	41 antibiotics + spirohexenolide A	A bacterial cytoprofiling technique (BCP) has been developed to identify the mechanism of action of antibiotics. The mechanism of action of spirohexenolide A has been elucidated.
2015	[59]	[19]	FM4–64, SYTOXGreen, DAPI	*Acinetobacter baumannii* ATCC 19606	cecropin A	Cecropin A rapidly kills bacteria by disrupting membrane integrity.
2015	[60]	[19,29]	FM4–64, SYTOXGreen, DAPI	*B. subtilis* 168	A number of naphtyl and biphenyl synthetic compounds (FtsZ inhibitors)	Among tested compounds, one exhibited the clear effect on cell division. Others have an action on bacterial membranes, in addition to targeting FtsZ.
2015	[61]	[19]	FM4–64, SYTOXGreen, DAPI	*A. baumannii* AB5075 (MDR)	Combinations of azithromycin with other antibiotics	Azithromycin could act synergistically with colistin. Main mechanism of action retains the same – protein synthesis inhibition.
2015	[62]	[19]	FM4–64, SYTOXGreen, DAPI	*E. coli* ATCC 25922	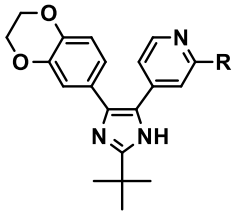 R = H or Me	Pyridineimidazoles cause morphological changes similar to those caused by globomycin (inhibitor of lipoprotein transport to the outer membrane).

2015	[63]	[19]	FM4–64, SYTOXGreen, DAPI	*E. coli* ATCC 25922 Δ*tolC*	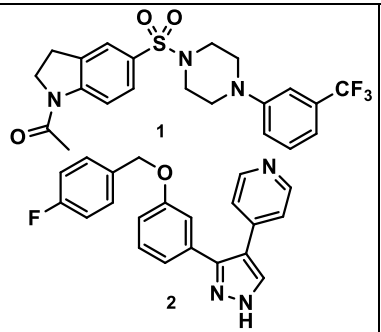	Both compounds gave distinctly different morphologies, despite the fact that each inhibits a component related to cell wall biogenesis. **2** affects membrane integrity.
2016	[29]	-	FM4–64, SYTOXGreen, DAPI	*B. subtilis* PY79 and transformants	Several standard antibiotics and 4 non-steroid anti-inflammatory drugs with antibacterial activity	Rapid Inhibition Profiling (RIP) was described. It's a system for creating cytological profiles of new antibiotic targets for which there are currently no chemical inhibitors. RIP consists of the fast, inducible degradation of a target protein followed by BCP.
2016	[64]	[19,29]	FM4–64, DAPI, FtsZ-GFP	*B. subtilis* 168, *B. subtilis* SU570 (FtsZ-GFP)	12 FtsZ inhibitors	2 distinct cytological profiles caused by selected cell division inhibitors were described.
2016	[65]	[19]	FM4–64, SYTOXGreen, DAPI	*Escherichia coli lptD4213*	*B. subtilis* 3610 extract	BCP was used for activity-guided purification of molecules with different activities. Translation inhibitors (bacillaenes) and membrane permeabilizers (plipastatin, subtilosin and SKF) were identified in the extract by the method.
2016	[66]	[18,19]	FM4–64, SYTOXGreen, DAPI	*E. coli* NR698 (*lptD*)	stenothricin, stenothricin-GNPS	Although structurally related, stenothricin and stenothricin-GNPS have different effects on bacterial cells.
2016	[67]	[19]	FM4–64, SYTOXGreen, DAPI	*E. coli* MC4100 (*lptD4213*)	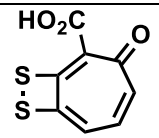 **Tropodithietic acid**	Tropodithietic acid operates like nigericin to disrupt the proton motive force across the cell membrane

2017	[68]	[19]	FM4–64, SYTOXGreen, DAPI	*E. coli* MC4100 (*lptD4213*)	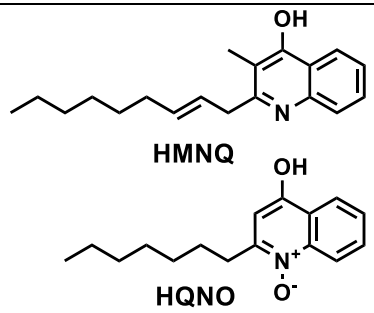 HMNQ HQNO	HQNO and HMNQ gave different phenotypes: HQNO exhibited a unique cytological profile, while HQNO are similar with membrane disruptors.
2017	[69]	[18,19, 29]	FM4–64, SYTOXGreen, DAPI	*Bacillus subtilis* PY79	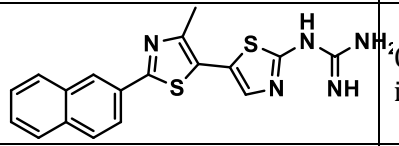	Compound inhibits cell wall biosynthesis in *Bacillus subtilis*.
2017	[70]	[18,19, 29]	FM4–64, SYTOXGreen, DAPI	*Bacillus subtilis* PY79, *E. coli ΔtolC*	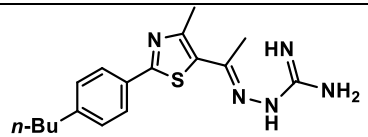	Compound exerts its antibacterial activity by inhibiting cell wall synthesis.
2017	[71]	[19]	none	E. coli ATCC 25922, A. baumannii ATCC 17978, Pseudomonas aeruginosa PAO1	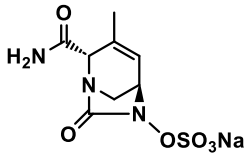 ETX2514	PBP2 inhibition is the probable mechanism of the antibacterial activity of ETX2514 versus Enterobacteriaceae.
2017	[72]	[19]	FM4–64, SYTOXGreen, DAPI	*Escherichia coli* MC1061 pBAD and pBAD:Gp2	Bacterial RNA polymerase	Gp2 mediated dysregulation of RNA polymerase activity results in a biphasic growth pattern.
2017	[73]	[18,19, 29]	FM4–64, SYTOXGreen, DAPI	Bacillus subtilis PY79	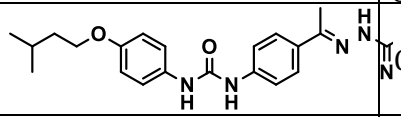	Compound inhibits cell wall synthesis
2018	[74]	[19]	FM4–64, DAPI	*E. coli* BW25113 ΔtolC, *Caulobacter crescentus* CB15N	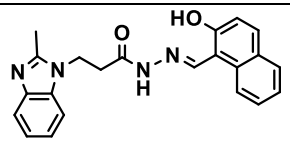	Compound arrests cytokinesis during late stages of bacterial cell division. The phenotype differs from other cell wall inhibitors.
2018	[75]	[18,19, 29]	FM 4–64, DAPI, SYTOX Green	*Bacillus subtilis* PY79 and transformants	Bacterial enzymes involved in pyrimidine nucleotide biosynthesis (thymidylate	Degradation of enzymes involved in the deoxyribonucleotide synthesis branch of the pathway (NrdF, TMK) specifically

					kinase TMK, cytidylate kinase CMK, and β-subunit of the ribonucleoside-diphosphate reductase NrdF)	affects DNA replication as expected. Degradation of CMK, which is involved in the synthesis of both ribonucleotides and deoxyribonucleotides, produced a complex cytological profile that could be recapitulated by simultaneous inhibition of DNA replication and WTA synthesis.
2018	[76]	[19]	FM1-43fx, DAPI	*E. coli* NB27001	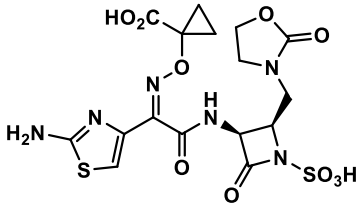 LYS228	LYS228-induced phenotypic profile is similar to aztreonam-induced (PBP3 inhibitor).
2018	[30]	-	Nile red, DAPI	*E. coli* CFT073, *E. coli* MG1655 (K-12), *E. coli* CFT073 *lptD*(*imp4213*)	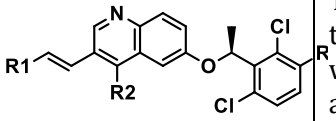 G592 R1 = -CO_2H, R2 = H, R3 = F G913 R1 = -CO_2H, R2 = cyclopropyl, R3 = G332 R1 = 1*H*-tetrazol-5-yl, R2 = cyclopropyl,	The msbA conditional knockout transformants of *E. coli* were obtained. It was used as a control strains for analyzing the MsbA-deficient phenotype. 3 synthetic quinoloines were identified as selective MsbA inhibitors by phenotypic screening.
2018	[77]	[19]	FM 4–64, DAPI, SYTOX Green	*E. coli* MC4100 *lptD4213*	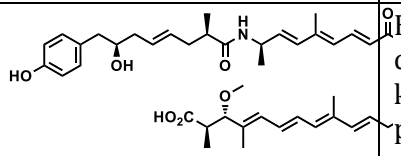 Thailandamide A	Bacterial cytological profiling and comparison with ten antibiotics with known modes of action revealed a unique profile for thailandamide, suggesting a distinct mechanism of inhibition.
2018	[78]	[19]	Hoechst 33342, FM 4–64	*A. baumannii* 1408 (MDR)	Tachyplesin III (antimicrobial peptide)	Tachyplesin-induced phenotype is similar with lipid synthesis inhibition.
2018	[79]	[19]	FM 4–64, DAPI, SYTOX Green	*B. subtilis* PY79 E. coli K1	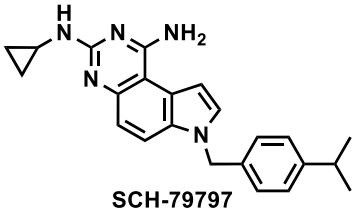 SCH-79797	The morphological similarity between cells treated with SCH79797 and polymyxin B, especially under osmotically stabilizing conditions, indicates that SCH79797 acts as a membrane-active compound.

2018	[31]	-	FM4-64, Hoechst 33342	*E. coli* BL21(DE3) pCWori-Dendra2	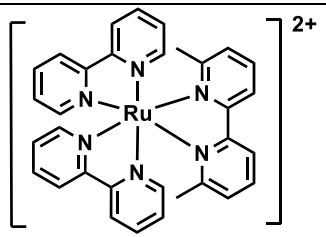 $[Ru(bpy)_2(dmbpy)]^{2+}$	An approach to mechanism of action studies for potential anticancer compounds was developed by utilizing the simple prokaryotic system, *E. coli*, and its utility was demonstrated with the characterization of a ruthenium complex $[Ru(bpy)_2(dmbpy)]^{2+}$.
2018	[41]	-	GFP-labelled proteins: RecA (DNA-repairing enzyme), DnaN (DNA polymerase subunit), RpoC (RNA polymerase subunit), and RpsB (ribosomal subunit)	*B. subtilis* 168 transformants	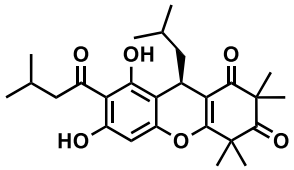 rhodomyrtone	The cellular localization of none of GFP-labelled proteins was affected by rhodomyrtone, indicating that the compound does not inhibit any of these intracellular processes (DNA reparation, DNA replication, RNA synthesis, protein synthesis)
2018	[80]	[19]	FM4-64, SYTO-9	*Salomella enterica* subsp. *enterica* serotype Typhimurium	4 synthetic compounds (SM1, SM3-5)	Compounds alter *Salmonella* cell membrane and cell wall integrity
2018	[81]	[19]	FM4-64, SYTO-9	*E. coli* O78 (avian pathogenic)	11 synthetic compounds	Compounds affect bacterial cell membrane. Treated bacteria showed membrane disrupted morphology along with formation of membrane defects.
2019	[47]	[19]	Wheat germ agglutinin-tetramethylrhodamine, Alexa-488-conjugated rabbit anti-FtsZ antibody	*B. subtilis* JH642	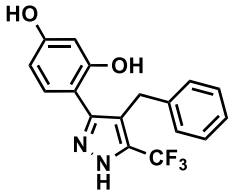 Min-1	Min-1-treated cells of *B. subtilis* exhibit unique phenotype (reduced length).
2019	[82]	[19]	FM4-64FX, Hoechst 34580, SYTO-9	*E. coli* BW25133	13 beta-lactams, NXL105 (PBP2 inhibitor) and cycloserine	Deep profiling of cell wall inhibitors revealed the identification not only mechanism but main target.

2019	[48]	[19]	FM1-43, propidium iodide (PI) FM4-64, WGA- Alexa Fluor 488	*S. aureus* ATCC 25923, *B. subtilis* PY79	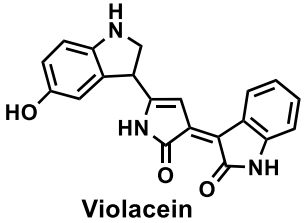 Violacein	Violacein quickly permeabilizes bacterial cells. Cell permeabilization was accompanied by the appearance of visible discontinuities or rips in the cytoplasmic membrane, but it did not affect the cell wall.
2019	[83]	[19]	FM 4-64, DAPI, SYTOX-Green	*A. baumannii* ATCC 19606, ATCC 17978, *E. coli* AD3644 (Δ*tolC*)	22 antibiotics	BCP was implemented for *A. baumannii*. BCP platform can distinguish among six major antibiotic classes and can also subclassify antibiotics that inhibit the same cellular pathway but have different molecular targets. BCP was used to show that the compound NSC145612 inhibits the growth of *A. baumannii* via targeting RNA transcription.
2019	[84]	[19]	FM4-64, DAPI, SYTOX-Green	*A. baumannii* AB5075 (MDR)	Combination of azithromycin and minocycline	BCP demonstrates augmented translation inhibition in MDR *A. baumannii* upon antibiotics co-treatment
2019	[85]	[19]	FM 4-64, DAPI, SYTOX-Green	*E. coli* ATCC 25922	2 synthetic biotin carboxylase inhibitors	Novel bacterial biotin carboxylase inhibitors showed similar phenotypic profile like the known compound 1.
2019	[49]	[19]	FM4-64FX, DAPI	*Clostridium perfringens* ATCC 13124	Ruminococcin C1 (antimicrobial peptide)	Ruminococcin treatment leads to three morphotypes identical to the ones induced by metronidazole.
2019	[86]	[19]	FM4–64, SYTOXGreen, DAPI	*Staphylococcus aureus* D712 (MRSA, VISA)	nafcillin	The effect of nafcillin at various sub-inhibitory concentrations were monitored using BCP
2019	[87]	[19]	FM4–64, SYTOXGreen, DAPI	*B. subtilis* 6051, *E. coli* ATCC 25922	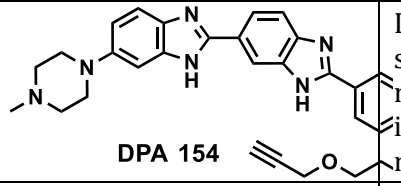 DPA 154	DPA 154 causes induction of spheroplastic phenotypes with additional membrane damage. It's a DNA synthesis inhibitor with a second membrane-active mechanism of action.
2019	[33]	[19]	FM4–64, SYTOXGreen, DAPI	*E. coli* BW25113, *A. baumannii* ATCC	ca. 10 000 compounds from the Roche pharma	The semi-automated bacterial phenotypic fingerprint (BPF) profiling platform in

				17978	compound library	conjunction with a machine learning-powered dataset analysis was used for screening and prediction of compounds' mode of action. The method identifies weak antibacterial hits allowing full exploitation of low potency hits frequently discovered by routine antibacterial screening. BPF classification tool can be successfully used to guide chemical structure activity relationship optimization, enabling antibiotic development and that this approach can be fruitfully applied across species.
2019	[88]	[19,49]	FM4-64FX, DAPI	*Clostridium perfringens* ATCC 13124	Enniatins and beauvericin (antimicrobial peptides)	Results showed that in *C. perfringens*, enniatins A and A1 (mainly containing *sec*-butyl groups) act like Rifampicin by causing an inhibition of the synthesis of RNA, whereas enniatins B, B1, and beauvericin (mainly containing *iso*-propyl or phenylmethyl groups) act like Tetracycline by inhibiting the synthesis of proteins.
2020	[89]	[19]	FM4–64, SYTOXGreen, DAPI	*E. coli* ATCC 25922	Clavanin A (antimicrobial peptide), combination with Zn^{2+}	Clavanin A at neutral pH interacts with the membrane, while combination with Zn^{2+} at acidic pH reveals unique photypes.
2020	[90]	[19]	none	*E. coli* ARC2687 (bla_{AmpC}, $bla_{CTX-M-14}$)	Cefpodoxime, ETX1317 and combination	Exposure to ETX1317 caused normally rod-shaped *E. coli* to become spherical, a morphology associated with PBP2 inhibition. Exposure to cefpodoxime (PBP1a/b and PBP3 inhibitor) induced cell elongation. Treatment with a combination of cefpodoxime and ETX1317 resulted in a complex "beads on a string" phenotype, demonstrating multi-PBP inhibition.

2020	[91]	[19]	FM4–64, SYTOXGreen, DAPI	*E. coli lptD4213*	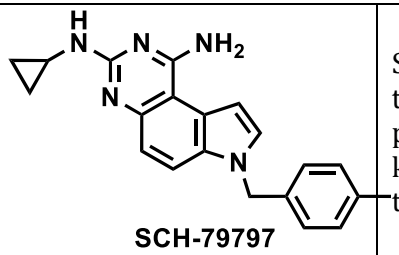 SCH-79797	SCH-79797 clusters closely to the co-treatments (trimethoprim with nisin or polymyxin B). It indicates that SCH-79797 kills bacteria by targeting both DHFR and the membrane.
2020	[50]	-	none	*Mycobacterium smegmatis* ParB-mCherry	12 antimycobacterial compounds	The morphotype database of *M. smegmatis* essential gene knockdown mutants was created using CRISPR interference approach. The morphoprofiling method was validated using 12 compounds with known targets.
2020	[92]	[19]	Sytox Green, FM4-64, DAPI	*E. coli* ATCC 25922, *M. smegmatis* mc²155	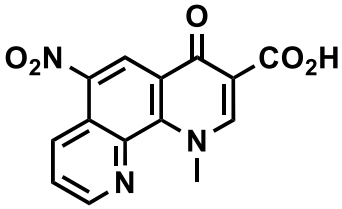	Compound exhibits the same phenotype as ofloxacin.
2020	[93]	[19]	Sytox Green or NBD-azithromycin, FM4-64, DAPI	*Achromobacter xylosoxidans* Florida (MDR)	azithromycin	Azithromycin is acive against bacteria in physiology-relevant medium and has enhanced entry into bacterial cells.
2020	[94]	[19]	FM4-64FX, DAPI	*E. coli* ATCC 25922, *B. subtilis* RPT 44	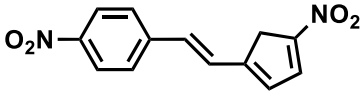 IITR06144	IITR06144-treated cells exhibited a strong filamentation phenotype, which is indicative of the SOS response.
2020	[51]	[19]	SYTO-24, FM4-64FX	*M. tuberculosis* Erdman	34 antibiotics + 3 synthetic compounds	Rapid profiling platform called Morphological Evaluation and Understanding of Stress (MorphEUS) was developed for *M. tuberculosis*. Using MorphEUS, we identified secondary effects for moxifloxacin and bedaquiline.
2020	[95]	[19]	FM4–64, SYTOXGreen, DAPI	*Vibrio parahaemolyticus* AHPND	vibriophage Seahorse	phage Seahorse likely inhibits protein translation of bacteria at the early stage of infection

2021	[96]	[19]	FM4–64, SYTOXGreen, DAPI	*B. subtilis* ATCC 6633	gausemycin A	Gausemycin A exhibits profile similar with daptomycin.
2021	[97]	[19]	FM4-64, SYTO-9	*E. coli* APEC O78	3 Lactobacillus rhamnosus GG-derived peptides	In P1-, P2-, and P3-treated APECs, no or minimally visible membranes were observed, suggesting that peptides disrupted bacterial membrane.
2021	[98]	[19]	FM4–64, SYTOXGreen, DAPI	*S. aureus* ATCC 29213, *B. subtilis* PY79	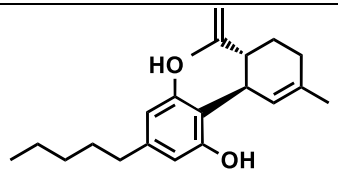 cannabidiol	BCP gave results consistent with membrane permeabilization action of cannabidiol.
2021	[99]	[19]	FM4–64, SYTOXGreen, DAPI	*B. subtilis* PY79	*S. felis* C4 extract and micrococcin P1	*S. felis* C4 extract and micrococcin P1 showed greater elongation compared to DMSO control and nucleoids that were highly condensed into toroidal structures, a characteristic of compounds that block translation, such as tetracycline.
2021	[100]	[19]	FM4–64, SYTOXGreen, DAPI	*S. aureus* D592 and D712	vancomycin	Bacteriological (cation-adjusted Mueller-Hinton broth) as well as physiological (R10LB) media was used to determine the effect of vancomycin on USA100 strains.
2021	[101]	[19]	FM4–64, SYTOXGreen, DAPI	*E. coli* JP313 Δ*tolC*	9 derivatives of 5-benzylidenethiazolidine-2,4-dione	Compounds inhibited two distinct metabolic processes, DNA replication and cell wall biogenesis. Compound 13 induced membrane permeability and cell lysis with no sign of inhibited DNA replication. This compound had a relatively high MIC compared to most other active molecules. In addition to nonspecific inhibitors, we identified three molecules (compounds 9, 11, and 27) that selectively inhibited DNA replication.
2021	[34]	-	FM4–64, SYTOXGreen,	*K. pneumoniae* NCTC	9 known antibiotics	High-content imaging (HCI) technique for

			DAPI	43816, *S. typhimurium* NCTC 13348, *S. aureus* ATCC 29213		phenotyping bacteria under antimicrobial exposure at the scale of individual bacterial cells was developed. Novel analysis pipelines were established for both Gram-negative bacilli and Gram-positive cocci.
2021	[35]	[34]	Alexa Fluor 647-labeled polyclonal antibody to the *Salmonella* common structural antigens (CSA), DAPI, SYTOXGreen	*S. typhimurium* isolates SL1344 (ST19, United Kingdom), VNS20081 (ST34, Vietnam), D23580 (ST313, Malawi)	ciprofloxacin	Ciprofloxacin exposure drives the formation of discrete bacterial populations of variable lengths.
2021	[102]	[19]	FM4-64, DAPI	*E. coli* BW25113 and Δ*mdtK*	Co-culture of bacteria with *Penicillium* sp. str. 12 or SAM3	Experiments showed that effect of co-cultivation is similar to that of antibiotics that target cell wall biosynthesis, such as mecillinam and amoxicillin.
2021	[103]	[19]	none	*P. aeruginosa* PAO1	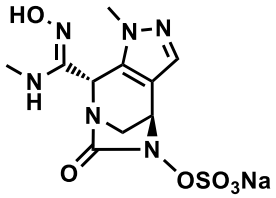 ETX0462	The morphology of treated cells is consistent with previously described phenotypes for PBP2-selective inhibition.
2022	[104]	[18]	FM5-95, DAPI	*B. subtilis* 168	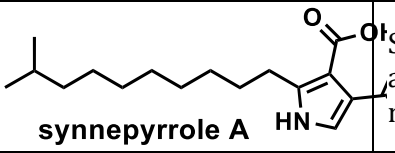 synnepyrrole A	Synnepyrrole A compromises the function and integrity of the bacterial cytoplasmic membrane.
2022	[32]	-	Hoechst 34580, FM4-64FX	*E. coli* BW25113	33 antimicrobials and combinations	The patterns of morphological change, including morphological potentiation, competition, and the emergence of unexpected morphologies were identified. These frequently did not correlate with synergistic or antagonistic effects on viability, suggesting

						morphological approaches may provide a distinctive signature of the biological interaction between compounds over a range of conditions
2022	[105]	[19]	FM4–64, SYTOXGreen, DAPI	*P. aeruginosa* PAO1 and phage-resistant mutants AM.P2-X-1, Mat-X-1, Kat-X-2	LL-37 (antimicrobial peptide)	The LL-37-treated mutants had significantly increased SYTOX Green staining compared to PAO1 indicating the increased antimicrobial peptide susceptibility.
2022	[106]	[19,82]	FM4–64, SYTOXGreen, DAPI	*K. pneumoniae* KPM1026a, *A. baumannii* ATCC 17978, *P. aeruginosa* PAM1154	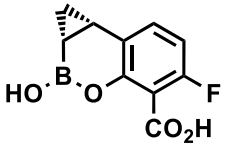 **Xeruborbactam (QPX7728)**	Xeruborbactam-induced changes in cellular morphology are consistent with inhibition of multiple PBPs
2022	[45]	[19,64]	FtsZ-GFP	*B. subtilis* SU570 (FtsZ-GFP)	12 FtsZ inhibitors	BCP was used for target validation of synthetic FtsZ inhibitors.
2022	[36]	-	Ffh-mVenus, FtsY-mVenus, uL1-mVenus	*Shewanella putrefaciens* CN-32 and transformants with Ffh-mVenus, FtsY-mVenus, uL1-mVenus	puromycin, rifampicin, chloramphenicol	Antibiotic Drug screening and Image Characterization Toolbox (A.D.I.C.T.) workflow was developed. It covers aspects of experimental setup deployment, data acquisition and handling, image processing (e.g. ROI management, data transformation into binary images, background subtraction, filtering, projections) as well as statistical evaluation of the cellular stress response (e.g. shape measurement distributions, cell shape modeling, probability density evaluation of fluorescence imaging micrographs) towards antibiotic-induced stress, obtained from time-course experiments.

2022	[107]	[19]	FM4–64, SYTOXGreen, DAPI	*S. aureus* BH1-CC (MRSA)	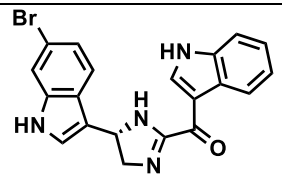 (-)-spongotine A	The MOA of (-)-spongotine A is linked to membrane permeation and disruption.
2022	[108]	[19]	FM4–64, SYTOXGreen, DAPI	*E. coli* CGSC 4213 (ΔlptD, LPS-deficient), *B. subtilis* NR-607	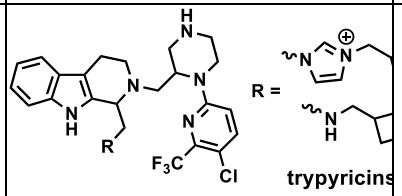 trypyricins	Obtained phenotypes are highly similar to those induced by daptomycin.
2022	[109]	[19]	FM4-64FX	*M. tuberculosis* H37Rv mc^{2}6020	evybactin	*M. tuberculosis* cells treated with evybactin were approximately two times longer than non-treated cells. This morphological change is typically observed in bacteria treated by DNA synthesis inhibitors, FtsZ inhibitors and β-lactams
2022	[110]	[19]	FM4–64, SYTOXGreen, DAPI	*P. aeruginosa* PAO1	mecillinam, meropenem, piperacillin and ceftazidime	*P. aeruginosa* treated with these antibiotics have morphological differences based on the PBP of the antibiotic targets
2022	[111]	[19]	FM4–64, SYTOXGreen, DAPI	*E. coli* JP313 Δ*tolC*	4 *Streptomyces* soil isolates	*E. coli* cells incubated adjacent to each of the four *Streptomyces* isolates displayed characteristic cytological profiles that, in some cases, allowed for the classification of these strains according to the MOA of the natural products they produced.
2022	[112]	[19]	FM4–64, SYTOXGreen, DAPI	*E. coli lptD4213*	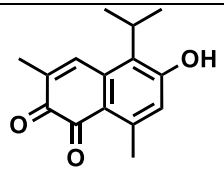 mansonone G	Mansonone G displays rapid membrane permeabilizing activity

2022	[39]	-	FM4-64, SYTO-9	*B. subtilis* 168	14 known antibacterials	Quantitative time-lapse fluorescence imaging method, Dynamic Bacterial Morphology Imaging (DBMI) was developed to facilitate the process of antimicrobial MoA identification.
2022	[44]	[18,19]	HbsU-GFP, WALP23-mCherry	*B. subtilis* 168CA-CRW419	tatiomycin	The cytoplasmic membrane was unaffected unlike in the control compound nisin, which forms large pores in the membrane. Treatment with tatiomicin induced chromosome decondensation, similar to the effects elicited by the RNAP inhibitor rifampicin
2022	[113]	[19]	FM4–64, SYTOXGreen, DAPI	*B. subtilis* ATCC 6051	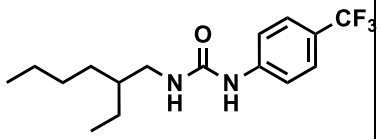	While the BCP analysis clearly shows that compound acts through a membrane-related mechanism, it is apparent that its mode of action is not the same as calcimycin.
2023	[114]	[19]	FM4–64, SYTOXGreen, DAPI	*V. parahaemolyticus* EB101 and AHPND	vibriophage KVP40, lytic transglycosylase (LT) and mutant protein E80A-KVP40-LT	Upon vibriophage KVP40 infection, *V. parahaemolyticus* exhibited morphological changes similar to those observed when treated with mecillinam. Heterologous expression of wild-type KVP40-LT induced similar bacterial morphological changes to those treated with the whole phage or mecillinam, prior to cell burst. On the contrary, neither the morphology nor the viability of the bacteria expressing signal-peptide truncated- or catalytic mutant E80A-KVP40-LT was affected.
2023	[43]	[19]	FM4-64, DAPI, NG-GlpT	*E. coli* W3110, *B. subtilis* DSM402, *E. coli* BCB472	38 *N*4-substituted piperazinyl norfloxacin derivatives	Phenotypic analysis of both *E. coli* and *B. subtilis* confirmed a typical gyrase inhibition phenotype for all of the tested compounds. Assessment of possible additional targets revealed three compounds with unique effects on the *B.*

						subtilis cell wall synthesis machinery, suggesting that they may have an additional target in this pathway. Comparison with known cell wall synthesis inhibitors showed that the new compounds elicit a distinct and, so far, unique phenotype, suggesting that they act differently from known cell wall synthesis inhibitors. Interestingly, our phenotypic analysis revealed that both norfloxacin and ciprofloxacin displayed additional cellular effects as well, which may be indicative of the so far unknown additional mechanisms of fluoroquinolones.
2023	[42]	[19]	FM4-64, DAPI, GFP-GlpT	*E. coli* BCB472, *E. coli* W3110	7 *N*4-substituted piperazinyl amino acid derivatives of norfloxacin	Gyrase inhibition could be confirmed for 4 compounds, but not for 3 others. No membrane aberrations were observed in the FM4-64 membrane stain. To confirm that there are no additional effects on the cytoplasmic membrane, a GFP fusion to the ubiquitous membrane protein GlpT was used as a proxy for the inner membrane (strain BCB472), and indeed no effects were observed
2023	[115]	[19]	FM4-64, DAPI	*E. coli* O157:H7	2 functionalized chickpea-derived Leg2 antimicrobial peptides	The formation of "ovoid cells" with condensed nucleoid was detected. It could be linked with peptidoglycan synthesis inhibition.

2023	[116]	[19]	FM4–64, SYTOXGreen, DAPI	*A. baumannii* ATCC 17978	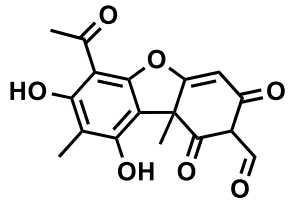 usnic acid	A high-resolution BCP method that can capture morphological variations of bacteria upon antibiotic treatment was developed. MOA classification accuracy is above 90%. Combinations of two antibiotics induce altered cell morphologies that could be deconvoluted. The method successfully revealed multiple cytological changes caused by a natural product that, by itself, is inactive against *A. baumannii* but synergistically exerts its multiple antibacterial activities in the presence of colistin.
2023	[117]	[19]	FM4–64, SYTOXGreen, DAPI	*B. subtilis* ATCC 23857	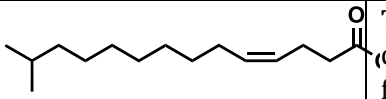 (Z)-13-methyltetradecen-4-oic	The fatty acid was found to rapidly destabilize the cell membrane by pore formation and membrane aggregation in *B. subtilis*
2023	[118]	[19]	SYTO-9, Propidium iodide	*E. coli* BW25113	psi-capsids (antimicrobial peptides)	The new approach was developed based on time-lapse microscopy with microfluidics to investigate the concentration-dependent killing kinetics of stationary-phase bacterial cells. The psi-capsids killed cells by disrupting their membranes at all concentrations tested
2023	[119]	[19]	FM4-64, DAPI	*P. aeruginosa* K2733 (PAO1 ΔmexB, ΔmexX, ΔmexCD-oprJ, ΔmexEF-oprN)	Combinations of antibiotics and phage ΦKZ	The MoA-specific interactions between antibiotics and phage ΦKZ infection were identified. Some classes of antibiotics strongly inhibited phage replication, while others had no effect or only mildly affected progression through the lytic cycle.
2023	[46]	[19]	FM4-64, DAPI, GFP-GlpT	*E. coli* W3110, *E. coli* BCB472	19 derivatives of norfloxacin	BCP confirmed inhibition of DNA synthesis for all except two tested derivatives. Further phenotypic analysis revealed polypharmacological effects on

						peptidoglycan synthesis for four derivatives.
2024	[120]	[19]	FM4-64, DAPI	*E. coli* CCUG31246	3 antimicrobial peptides	The peptides' cytological profiles similar to polymyxin B.
2024	[121]	[19]	Nile Red, DAPI	*B. subtilis* PrpsD-GFP, *B. subtilis* MinD-GFP	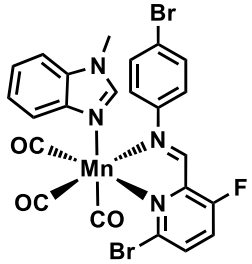 MnG9MeBeIm	Compound targets the bacterial membrane without inducing pore formation or depolarisation
2024	[40]	[39]	FM4-64, SYTO-9	*B. subtilis* 168	harzianic acid	Harzianic acid exhibited the phenotype similar with nisin. The result obtained from DBMI method.
2024	[122]	[19]	Nile red, DAPI	*B. subtilis* 168CA	valinomycin, vancomycin, nisin	A minimal set of accessible phenotypic assays that allow distinction between membrane and cell wall targets and identification dual-action inhibitors was tested. It should include a membrane-potentiometric probe, and fluorescent protein fusions to MinD and MreB as basic assay set and Laurdan-based fluidity measurements and a PliaI reporter fusion as a recommended extention.